STRUCTURAL HEALTH MONITORING OF TRUSS STRUCTURES USING STATISTICAL APPROACH

Mahdi Saffari Farsani

A Thesis

in

the Department of

Mechanical and Industrial Engineering

Presented in Partial Fulfilment of the Requirements
for the Degree of Master of Applied Science (Mechanical Engineering) at
Concordia University
Montreal, Quebec, Canada

December 2013

ABSTRACT

Structural Health Monitoring of Truss Structures

Using Statistical Approach

Mahdi Saffari Farsani

Structural Health Monitoring (SHM) has drawn attention of many researchers recently. The reason is its huge effect on reduction in maintenance costs as well as increasing reliability of mechanical devices.

In this thesis the concept of SHM is explained and a damage detection methodology is proposed using Auto Regressive (AR) parameters for truss type structures.

The AR parameters of a healthy case are assumed to be the reference baseline data. A Damage Index is then defined to be the standard deviation of any other unknown signal from the baseline data. The proposed index provides an effective tool to detect the damage in the structure.

Sensor arrangement optimization has been performed as another part of this thesis which is a study on finding the optimum sensor arrangement to interrogate the most useful data given a limited number of sensors.

The localization process needs data classification techniques and has been conducted using Support Vector Machine (SVM) in this research for the first time. It is

shown that SVM can successfully classify different signals that are extracted from a 3D sample truss structure. This accomplished through generating large sets of simulated data forwarded to SVM tool to construct a Meta model which further is used to predict the unknown signals and find the most correlated "known" category and reports its case label as the best match for the "unknown" signal.

At the end, an extensive sensitivity analysis has been performed to study the effect of parameter changes to the detection and localization processes.

ACKNOWLEDGMENTS

I would like to acknowledge the following people who in some way contributed to the completion of this dissertation: My Father, Mansour, for teaching me the fundamentals of life skills, and scientific inquiry, and my mother, Ashraf, for instilling in me a confidence in everything I do. My mentors, Professor Ramin Sedaghati and Professor Ion Stiharu for training me how to ask the right questions and how to discover the important answers.

My student colleagues, especially Shahrzad Nouri, Walid Masoudi and Amin Changizi. Without their collaboration, my work would have been half as enriching and twice as boring. Finally I would like to thank my wife, Maedeh Heydari, for her years of unrelenting support and patience and dedicate this dissertation to her and my daughter Yasamin.

TABLE OF CONTENTS

LIST OF FIGURES

NOMENCLATURE

List of Abbreviations

SHM   Structural Health Monitoring

FRF   Frequency Response Function

MVPS   Mixed Variable Pattern Search (MVPS)

AR   Auto Regressive parameter

DI   Damage Index

SNR   Signal to Noise Ratio

List of Symbols

q Nodal displacement vector - $n \times 1$

$\dot{q}$ Nodal velocity vector - $n \times 1$

$\ddot{q}$ Nodal acceleration vector - $n \times 1$

$f(t)$ Dynamic force input signal

u Input vector - $s \times 1$

y Output vector

U Input vector in frequency domain

Y Output vector in frequency domain

M   Mass matrix - $n \times n$

D   Damping matrix - $n \times n$

KStiffness matrix $-n \times n$

B_o Input force matrix - $n \times s$ – position of input excitation force

C_a Output acceleration matrix - $r \times n$- position of desired sensor locations

ρ Density

A   Truss structure cross section area

L   Truss member length

x   Input state space vector

A, B, C, H   State Space representation matrices

ϕ_d , φ Mode shapes of damaged and corresponding pristine structures

l, m, n   Direction cosines of elements

f_i Frequency of mode *i*

$H_1(f)$ FRF of noisy output signal

$H_2(f)$ FRF of noisy input signal

$S_{uu}(f)$ Auto Spectral Density of the Input

$S_{yy}(f)$ Auto Spectral Density of the output

$S_{uy}(f)$ Cross Spectral Density of the Input and Output

p Damage intensity factor in optimization problem definition

$M \subset \{1,2,...,NN\}$ Subset of nodes indicating the sensor locations

$f(p,M)$ Objective function of optimization problem

$F_v(p)$ Full relative change of FRF of healthy and damaged cases (at all node locations)

$R_v(p,M)$ Reduced relative change of FRF of healthy and damaged cases (only at locations indicated by M)

$B(y^c, \varepsilon)$ open ball of radius $\epsilon > 0$ of y^c centered neighborhood

N_i Neighbor-1 set of M

$N(x)$ Sets of Neighbors (N_i)

μ_X Mean of data in vector X

$E(X)$ Mathematical expectation

σ_X Standard deviation

S Skewness

k Kurtosis

ϕ_j Auto Regressive parameters

p	AR model order
$\mathbf{X^T}$	Regressors
ε	Root Mean Squared Error (RMSE)
NR	Number of healthy state realizations
$A^{healthy}$	Cross section of healthy member
$A^{damaged}$	Cross section of damaged member

CHAPTER 1

INTRODUCTION

1.1   Motivation and objectives

Structural Health Monitoring (SHM) has attracted many researchers and engineers in many academic and technological centers and thousands of articles have been published in this area. The motivation to this huge effort in both universities and companies lies in several reasons like:

- Improving safety matters,

- Costs of inspection procedure,

- Probable significant damage in expensive structures due to failure in a small member,

- Man-hour required to do inspection,

- Monitoring and consequent costs and lots more.

 Also many scheduled and unscheduled maintenance and inspection operations are being done which cause ever increasing costs, in addition to indirect costs of overhauls

and not in service equipment. These conditions have guided scientists and engineers to seek for new solutions to reduce costs and time of inspections [1].

The objectives of this study are to address some of these concerns in the damage detection and localization phases in the truss structures. This study approaches to the problem statistically as one of the existing tools in damage identification literature. The objectives of the current research could be summarized as:

- Finding a signal based SHM method to detect the damage in truss structures with the optimum number of installed sensors,

- Investigating about the optimum sensor placement in truss structures for a known damage location,

- Damage localization based on a training data pool and building a prediction Meta model to classify and categorize obtained signals and label them with the correct damage location.

- Sensitivity analysis of the proposed method and studying different parameter changes on the procedure performance

1.2 Literature review

The concept of SHM cannot be explained unless the definition of damage is introduced. Damage could be defined as any changes in the system that adversely affects its present or future performance. Damage is meaningful when two different states of a system are compared. One of which is assumed to be the reference state. The reference state is called also the healthy state or pristine state of the system [2]. The concept of damage is very diverse, and there are many different types of damages in different areas of technology.

For example, crack initiation in aircraft fuselage and body structures, are of major interest. Also fuel leak, over temperature, impact damage, bonding failure, composite delaminations, leading edge mass loss and corrosion are other usual damage types that are ranked from top to down in aircrafts [3]. In rotary equipment, shaft misalignment, rub or an undesired contact between rotary and stationary parts, shaft unbalance, shaft crack initiation and failure of rolling element bearing occur more frequently [4]. Therefore, to investigate the damage identification, one requires to clearly define the area of interest and type of damage encountered.

This literature review focuses on the study of structural and mechanical systems. In current study the damage is defined as any changes in material or geometrical properties such as system connectivity, cross section reduction and crack initiation or boundary condition that have any effect on system performance. In this literature review, a brief review of various methods of crack growth identification in structures using vibration based methods is provided. Vibration based methods rely on structure excitation, data acquisition and interpretation.

Damage identification of structures is one of the major sections of SHM and includes damage detection, localization, size estimation and calculating the rest of the structure life. Localization has different meanings depending on the context. For example isolation of a faulty member in a truss structure or the coordinate estimation of the damaged zone in an integrated structure like plate and shell [5]. Traditional Nondestructive Testing & Evaluation (NDT&E) techniques include dye penetration, radiographs, magnetic field, eddy current and acoustic or ultrasonic methods are in their

mature stages and currently are being used in different industries as inspection tools. These techniques have some limitations and disadvantages [6]:

- The affected zone must be estimated to a good extent prior test,

- The affected zone have to be accessible and out of reach areas may be remain untested,

- Methods may require the main equipment halted or a member removed from its position,

- Skilled worker is required to take reliable results,

- Sometimes damages only indicate their occurrence under working condition, and online, not offline.

To remove these limitations people are continuously seeking for better solutions to make structures more reliable and to make down times less as possible. SHM and consequently real time monitoring and damage identification needs data acquisition techniques in automated manner. Also fast enough algorithms are required to interpret obtained signals from sensors installed on the structures [7]. Figure 1-1 illustrates a comparison between SHM and NDT and also damage identification phases.
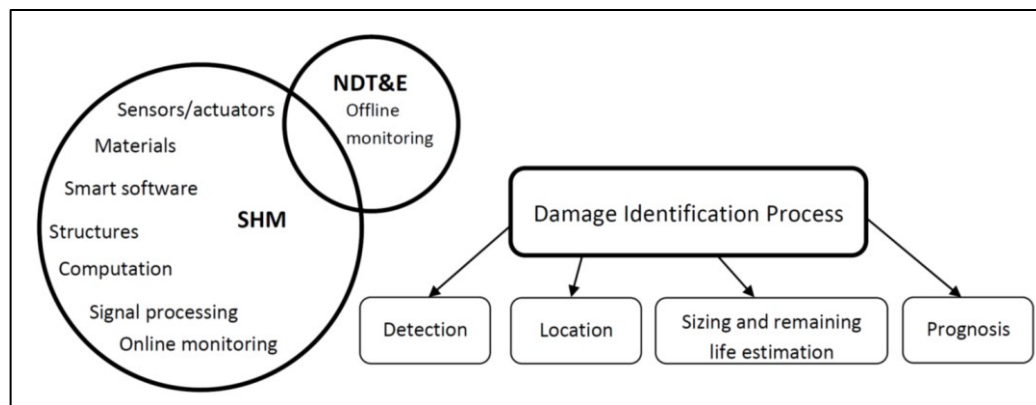
Figure 1-1: SHM, NDT&E and damage identification process overview [6]

1.3 Damage identification techniques

Damage identification includes detection, location, sizing and eventually prognosis. Several approaches have been into consideration to study these outlines which can be mainly classified into model based techniques and signal based techniques. Model based techniques require accurate modeling of the structure in both healthy and damaged status.

The model based techniques mostly rely on accurate finite element modeling and analysis. Model updating based damage identification [8-10], mode shape curvature and strain energy measurement are examples of model based damage identification process. On the other hand, signal based approach is also well developed. In this approach, structural excitation and sensor data measurement and interpretation are the tools to investigate and judge the structure status. Wave propagation, acoustic emission, wavelet and Fourier analysis are examples of signal based approach.

Figure 1-2 shows the general classifications for damage identification methods.
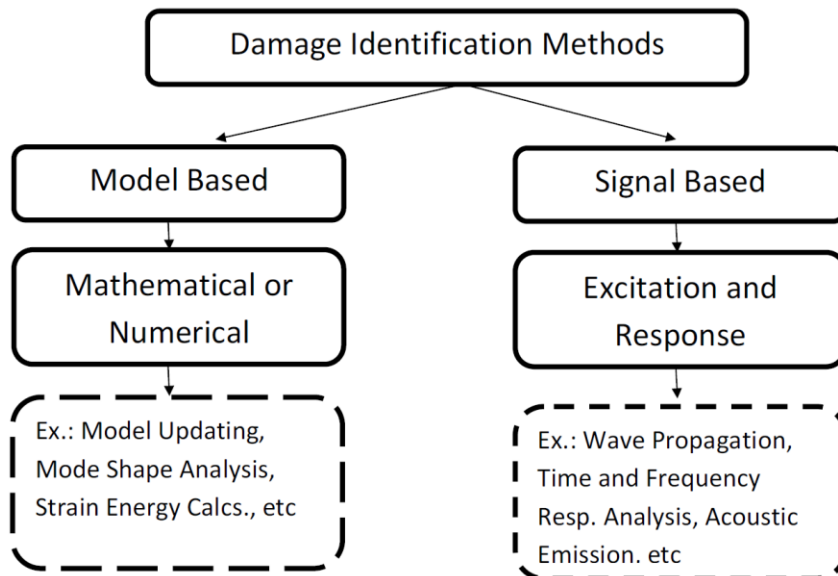
Figure 1-2: Distinction between model and signal based methods [6]

1.4   Modal analysis

Vibration based techniques usually use modal properties like frequencies, frequency response functions (FRF), mode shapes, damping ratios, transmissibility function and mode shape curvature methods to characterize damage in structures. When damage occurs in a structural member of a system it changes the dynamic properties of the system including stiffness, mass or damping which subsequently affect the modal parameters such as natural frequencies and mode shapes of the system. By correlating these changes to modal properties of the healthy structure one can diagnose the status of the structure. Damage is identified, when changes in modal properties is observed comparing to the healthy structure after testing a specimen [11-14].

Modal measurements are acquired by active or passive excitation. Active excitation uses actuators like PZT transducers or shakers while passive excitation, is the modal properties measurement using the system operational condition. For instance an aircraft is excited during landing due to impact exerted to the structure and so it bears passive excitation and no extra energy is required to interrogate the structure.

Usually cracks does not change mass and damping factor but they reduce stiffness of the structure to a plausible extent. In the following three important methods which utilizes the modal parameters for damage identification are briefly discussed.

1.4.1 Mode shape curvature method

Once the mode shapes of damaged and corresponding pristine structures are distinguished (ϕ_d, φ respectively), the curvature of every point i in the structure is numerically approximated as:

$$\varphi_i'' = \frac{\phi_{i+1} - 2\phi_i + \phi_{i-1}}{h^2}$$

Where h is the distance between the measurement points $(i+1)$ and $(i-1)$[15], The largest absolute computed difference between the mode shapes of the damaged and pristine structure is an indicator of the location of damage, $\delta\phi'' = |\varphi_d'' - \phi''|$. The main idea is that the second derivative or curvature of the mode shape is more sensitive to small perturbations than the mode shape itself. Also in beam and plate type structures the changes in curvature could be related to strain energy which is known as a sensitive damage indicator (see section 2.1.3). The largest value of $\delta\phi''$ could be an indicator for damage at a certain point [16].

1.4.2 Damage Index

A Damage Index is defined based on the changes of the jth mode curvature at location i

$$\beta_{i,j} = \frac{\left(\int_a^b \left[\varphi_j''^{d}(x)\right]^2 dx + \int_0^L \left[\varphi_j''^{d}(x)\right]^2 dx \right) \times \int_0^L \left[\varphi_j''(x)\right]^2 dx}{\left(\int_a^b \left[\varphi_j''(x)\right]^2 dx + \int_0^L \left[\varphi_j''(x)\right]^2 dx \right) \times \int_0^L \left[\varphi_j''^{d}(x)\right]^2 dx}$$

Where $\varphi_j''(x)$ and $\varphi_j''^{d}(x)$ are the second derivatives of the jth mode shape of pristine and damaged structures respectively. a (location i) and b (location $i+1$) denote

7

a portion of structure where damage is being studied. The second derivative of a mode shape in a location is exactly the same as acceleration of that point.

Typically a cubic polynomial curve fitting technique on measured data gives an estimation of mode shapes, and if more than one mode is employed, the DI will be the summation of each damage index corresponding to that mode

$$v_i = \sum_j \beta_{i,j}$$

Changes in the damage index and relating these changes with the potential locations are then assessed by statistical methods. Normal distribution of damage indices in different locations is extracted and DI values which are two or more standard deviation away from the mean DI value are reported to be most probable location of damage [17].

These methods were further extended utilizing Frequency Response Function (FRF) instead of mode shape data. It is claimed that this method can detect, localize and assess damage extent and the theory is fostered with some experimental results [7]. Nevertheless development of suitable damage metrics and identification algorithms is still a challenging issue for further research work. Damage index as a scalar quantity is a damage metric that gives a criterion to judge the extent of damage of a structure [5].

Although these methods are well applicable in some cases but are *not* applicable to the cases where sizes of cracks are very small relative to the structure, or the crack is somewhere in a wide area of the structure. The main reason is that small cracks do not change the modal properties noticeably, and thus they are not easily detectable using experimental methods. It should be noted that this limitation is not due to lack of sensitivity of the method, but it is due to the practical limitations of exciting higher modes. Normally lower modes do not change in a meaningful way, and on the other hand

excitation of higher modes requires high level of energy and usually is not viable in large structures like aircrafts or bridges. There are also other issues regarding higher mode excitation. Consider a truss with n elements, to excite the kth mode, around $k \times n$ sensors are required to install on the structure. Although some of the structural nodes are common and this may reduce the number of required sensors, it is still a problem of data acquisition and in reality it may confront many difficulties.

1.4.3   Strain energy and mode shape based damage detection

Damage occurrence alters the mode shapes more noticeable than natural frequencies. This fact attracted the interest of researchers; however this approach has its own drawbacks. Damage is a local matter and will not affect the lower mode shapes considerably while they are more accessible experimentally. Also the extracted mode shapes are under the influence of environmental conditions like ambient loads and sensor positioning and operational errors.

Mode shapes of structures store strain energy, and when the amount of this stored energy is high enough in a particular mode, the frequency and shape of that specific mode is highly sensitive to every change in stored energy in that specific mode. Hence tracking the changes in strain energy of the structure may be a good idea to indicate the damage location. The bending strain energy in a beam using classical beam theory in a particular mode shape is given by

$$U_i = \frac{1}{2}\int_0^l EI\left(\frac{d^2}{dx^2}\varphi_i\right)^2 dx$$

The required curvature for this equation is usually calculated numerically using the central difference estimation of mode shape displacements [18].

Modal Assurance Criterion (MAC) and Coordinate Modal Assurance Criterion (COMAC) are two common methods to compare mode shapes of pristine and damaged structures [1, 19]. MAC value is an indicator which denotes the similarity of two mode shapes from two different tests of a beam, say ϕ_A, ϕ_B in matrix form. These matrices have $n \times m_A$ and $n \times m_B$ elements respectively where n is the number of data points (sensors), m_A and m_B are numbers of modes in the respective tests. MAC value is then defined as

$$MAC(j,k) = \frac{\left(\sum_{i=1}^{n} \phi_{A_{ij}} \phi_{B_{ik}}\right)^2}{\sum_{i=1}^{n}\left(\phi_{A_{ij}}\right)^2 \times \sum_{i=1}^{n}\left(\phi_{B_{ik}}\right)^2}$$

$$j = 1,2,...,m_A \; ; \; k = 1,2,...,m_B$$

$$\phi_{A_{ij}} = i^{th} \; coordinate\, of\, the\, j^{th}\; column\; of\; \phi_A;$$
$$\phi_{B_{ik}} = i^{th} \; coordinate\, of\, the\, k^{th}\; column\; of\; \phi_B;$$

If MAC number is *one* then j^{th} mode of the first set and k^{th} mode of the second set are similar and if it is *zero* they are completely dissimilar.

As an example a bridge structure was tested before and after repair and MAC values for both situations were obtained, although the first seven natural frequency values were shifted by less than 3% respectively, the MAC value was different in a meaningful manner and it was concluded that comparing the MAC value is more convenient to judge the structure state than shifts in natural frequency [20-21].

COMAC value is a similar concept that compares a specific location in two sets of data point consisting of L modes, the summation will take place on j, k instead of i, so for location i and total modes of L it will be defined as [21]

$$COMAC(i) = \frac{\left(\sum_{j=1}^{L} \phi_{A_{ij}} \phi_{Bij}\right)^2}{\sum_{j=1}^{L} \left(\phi_{A_{ij}}\right)^2 \times \sum_{j=1}^{L} \left(\phi_{B_{ij}}\right)^2}$$

1.5 Impedance based methods

The mechanical impedance method has been introduced in the late 1970 and early 1980 and is based on measuring the response properties of forced excitation of structures. The excitation must be normal to the surface of the structure and is produced by conventional shakers and measured by velocity transducers. The transducer shall be a specialized one that measures the applied normal force and the induced velocity at the same time [22]. The mechanical impedance method is studied to be used as a non destructive testing (NDT) by Lange [23] and his work further extended by Cawley [24]. Cawley studied the bonded thin plates and suggested a method to find the disbonds. The impedance to excitation in the normal direction was predicted using the finite element analysis of vibrating bonded or disbonded thin plate.

The experimental work included installing a specialized transducer that measures the applied normal force and the induced velocity simultaneously, and then the impedance magnitude spectrum was compared with the finite element model. Some correlation with these two approaches has been derived to distinguish the presence of disbonds. These studies are the base of mechanical impedance method that is a non destructive evaluation (NDE) technique and is a dominant method to detect disbonds in laminated structures and delaminations inside composite members up to 6-mm depth. Ultrasonic mechanical impedance analysis (MIA) equipment are common in industry [5, 25-27].

1.6   Acoustic emission testing

Acoustic Emission (AE) has attracted attentions as a popular and powerful tool in NDT, condition monitoring, damage identification and structural health monitoring. This desire is partly due to recent advances in high speed digital waveform-based AE instruments which let a wide variety of AE waveform signals to be digitized and stored for analysis. However the main reason of the recent interests to AE is due to its ability to monitor a variety of machines and structures in a more holistic way. The major pivotal point in the direction of AE research trend came when work was carried out at an enhanced understanding of AE signal propagation in terms of guided acoustic modes, and this approach recently is designated as *Modal AE* and could be a departure point from conventional reliance on statistical analysis and significantly improves the knowledge about structural health monitoring capabilities using AE [28].

Traceability of results is often mentioned as the major deficit of AE testing, because AE measurements are dependent on many significant variables such as wave transmission, paths, sensor location and coupling, and sensor and system sensitivity. Also there are no measurement standards to estimate the real strength of AE source. This lack of standardization makes it very difficult to compare the results in different laboratories or on different structures[29].

AE testing is based on sensing the changes in signal strength due to sudden release of emitted energy. This energy emission is because of changing the stress field [30]. The amount of change order of magnitude could be referenced as an indicator of damage size, AE is suitable to scan a wide area and estimate the location of damage, and is known to be very sensitive to the external noise which limits its use in many applications.

1.7 Wave propagation Technique

Wave propagation methods use transducers for active sensing of a wave packet, and then the collected data via transducers must be interpreted by proper tools. Wavelets have been considered as one of these interpreting tools. Actually the presence of cracks can hardly be observed from the changes in modal parameters. Nevertheless these discontinuities may be detectable from the wavelet coefficient distribution. These coefficients could be obtained by the Continuous Wavelet Transform (CWT) or by digital signals which form the Discrete Wavelet Transform (DWT). Hence wavelet transform come into picture as a noticeable tool [31].

Conventionally, ultrasonic wave is employed to excite structures in order to interrogate for damage in a specimen. The ultrasonic wave is a high frequency acoustics wave and is applied by actuators to the structure. The traditional method of NDT solely identifies damage locally, using ultrasonic wave, excited by large transducers. Due to this issue it has limited application for SHM. The use of large transducers significantly increase the mass loading effects and besides, online monitoring of structures seems impossible using such large probes. Moreover it is not economically feasible. Instead, methods that could use wave propagation techniques with in-situ transducers are required [32].

Nowadays, researchers are seeking for more efficient solutions to eliminate the mentioned problems and wave propagation has proved itself to have this potential. The ideal solution includes [6, 33]:

- The ability to reach hidden and buried parts of structure.
- Propagation of waves to traverse direction and covering large distances.

For quick and efficient sweeping of whole structure to collect data

- Sensitivity to different types and sizes of damages.

Some types of damages do not affect structural dynamics properties and hence alternative methods should be sought with higher sensitivity to variation of system status.

- Consuming less excitation energy as possible.

Excitation of structures is one of the main issues for condition monitoring and lesser excitation energy would be a great advantage.

- Capable to be used for online condition monitoring.

Online inspecting of the structures requires fast and reliable data collection and interpretation algorithms. Fast data acquisition and processing and reliable decision making will lead to online monitoring that is a major step forward in structure condition monitoring.

Researchers have investigated the use of guided waves, particularly Lamb waves, for near real time condition monitoring [13, 34-35]. Lamb waves have great tendency to interfere on a propagation path (boundary or damage), and they travel over a long distance even in materials with high aspect ratio like carbon fiber reinforced composites [33]. Therefore a wide area, even hidden and out of reach parts can be easily scanned. The various types of damages that can be inspected by Lamb waves are discussed by Rose[36]. The main advantages of Lamb wave propagation method could be summarized as follow:

- The ability to inspect large structures even with coating and insulation.

- The ability to inspect whole cross sectional area of structural members.

- The least requirement of expensive tools and probes (insertion / rotation devices)

- It is not required to move the devices during inspection.

- Sensitive to multiple defects.

- Low energy consumption.

- Cost effectiveness.

As it could be seen, this approach of damage identification could be considered very close to the ideal solution that mentioned before. The Lamb wave based damage identification method is supposed to answer the following questions from easy to hard level[37]

- Has damage occurred in the structure?

- Where is the location of the damage?

- How much severe is the damage? Give a quantitative estimation.

- What is the remaining safe life of the structure?

1.8   Statistical pattern recognition approach

With a closer look to the problem of damage identification (detection, localization, life estimation) one may admire that it is intrinsically a pattern recognition problem. The reason is that it deals with categorization of present situation into damaged or healthy state. Saving the response signals of a given structure over time, enables us to have a good measuring meter using various statistical based pattern recognition techniques [38-39].

Time series method for structural health monitoring is evolving considerably among wider category of vibration based approach for SHM [40-45]. This approach uses response signals with or without random excitation. Then it requires a statistical model building, and finally a decision making procedure, to judge the current situation. Like every other vibration based method, this method relies on the fact that damages may cause some discrepancies in the system response which may be incorporated to detect the origin of perturbation.

There are many advantageous listed for statistical time series methods in the literature which some of them are [40]:

- Models are data based rather than physics based or finite element model which are elaborating

- Normal operation will not interrupt while assessing the system

- No requirement of modal models

- Statistical decision making based on previously gathered knowledge which encounters uncertainties inherently.

Some disadvantages of the statistical time series method:

- Since complete model of the structure is not employed the damage identification process is only to the point allowed by the incorporated model.

- Need for proper training, as the method is based on "enough" number of observations

- Potentially little physical interpretation of the damage nature

Statistical time series method uses random response signals from the structure in its healthy state and also from a number of probable damaged states, then by choosing the most suitable statistical model and extracting features out of signals (characteristic quantity); one would be able to characterize the structural state in each case. Among different statistical approaches some examples are [38]:

- Power Spectral Density (PSD) and Cross Spectral Density (CSD) based methods

- Frequency Response Function (FRF) based method

- Model parameter based method

- Residual (residual variance, likelihood function, residual uncorrelatedness) based methods

1.9   Optimal sensor placement on structures

Sensor types and placement on structures have a critical role in SHM. Sensor placement on structures usually is done either ad hoc or at last by experimentally testing few possible configurations and then selecting a set that performs the best. In this case, sensor placement relies on staff experience and available equipment [46].

If one can cast the sensor placement problem into an optimization problem then this problem can be handled more effectively. It would be more knowledge based rather than a random or experience based process. Having a limited number of sensors, the problem is to determine the number and location of sensors regarding an objective function[46].

Few literatures are available on sensor placement problem, specifically relating to SHM and damage identification. Staszewski et al. study this problem to detect and locate damage in composite materials[47], Shi et al. investigate optimal sensor placement strategy and prioritize the sensor location according to their ability to localize structural damage based on the eigenvector sensitivity method[48]. Gue et al. also study the global optimization using genetic algorithm technique [49].

1.10 Contributions of the thesis work

The significant contributions of this dissertation are summarized as follows:

1- A damage sensitive feature is found and a new Damage Index is proposed for the first time.

2- Support Vector Machine (SVM) as a classifier tool is used to localize damage in the structure, based on a previously built Meta model.

3- Sensitivity analysis is performed to figure out the effects of different parameters changes on the proposed SHM procedure. These parameters include number of sensors, crack size, excitation force location and some other parameters.

1.11 Thesis structure

This dissertation consists of 4 Chapters. The first Chapter is the introduction and literature review, where the latest techniques of SHM techniques in structures are discussed.

Chapter 2 discusses the modeling and methodology. The theories which are the backbone of the current study are developed in this Chapter. Nodal model and Finite Element formulation of truss structures are represented. Also system of second order differential equations is represented in State Space or first order equations where a systematic numerical solution for dynamic response analysis is proposed. In addition, generating of theoretical excitation force and Frequency Response Function is investigated. Sensor arrangement optimization problem in the truss structure is the subject of another section in this Chapter where the optimum sensor arrangement at nodal positions is found. Given a limited number of sensors and known damage location, the optimum arrangement is investigated. Damage Sensitive Features (DSFs) and Damage Index (DI) is also defined and represented in this Chapter. Finally damage localization using the Support Vector Machine (SVM) tool is proposed.

Chapter 3 includes the simulation results and discussion where the sensitivity analysis is also performed. Model validation is performed by comparing the ANSYS model with the written MATLAB code. DSFs and DIs are built and investigated for a specific example.

Chapter 4 is the final Chapter and includes the conclusion of the present research and further study proposal.

CHAPTER 2

MODELING AND METHODOLOGY

2.1 SHM procedure based on statistical pattern recognition

SHM in general is the process of detecting and localizing damages in structures in order to improve safety, reliability and maintenance costs. Here, SHM based on statistical pattern recognition approach has been effectively utilized to identify the damage in the truss type structures. Many structures normally are under repeated loading conditions. On the other hand, data acquisition and processing techniques are improving constantly. Hence statistical pattern recognition techniques can be cast as a powerful tool in the context of SHM.

The best arrangement of sensor locations is obtained by combining the developed finite element model of the structure and the Mixed Variable Programming Pattern Search (MVPS) algorithm. Then an optimization problem is formulated. The conditions to find the best arrangement are that the damage location as well as its severity should be known in advance. Otherwise this optimization problem does not have a unique solution. This problem is challenging because the objective function is computationally expensive

and first order derivatives are not available due to discrete nature of variables. The approach to solve the problem is numerical solution based on MVPS algorithm.

The proposed procedure to identify the damage using SHM based statistical pattern recognition technique has been summarized in the following steps.

1- Model the truss structure using the finite element method.

2- Generate a force signal with a controlled frequency content and amplitude

3- Introduce the generated force to the structure and find the dynamic response (acceleration) of the structure at sensor locations

4- Evaluate the damage sensitive features (DSF), build a baseline based on healthy states and compare the damaged states to the baseline

5- Build the damage sensitive matrix (DSM) and feed it to the Support Vector Machine (SVM) and complete the learning procedure and build a prediction model

6- Generate a test data base and introduce it to the trained model and find the localization accuracy

In the following subsections the theory and backbone of the above-mentioned steps are explained in detail and then in Chapter 3 the results are introduced and related discussions are made.

2.2   System modeling

System modeling is the most important section of any analytical data driven analysis approach. The objective of modeling is basically to develop a mathematical model which its response to various inputs is as close as possible to the reality. For simple geometry structural systems, analytical equations may be derived from physical laws, such as Newton's principles, Lagrange's equations, or D'Alembert's principle [50]. However for analysis of complex structural systems, numerical approach (mainly finite-element technique) is inevitable. Also system identification methods and test data may be utilized to build the model. The models could be either in time domain (differential equations), or in frequency domain (transfer functions).

In this research, the finite element technique has been employed to find the governing differential equations of the truss structure in the finite element format. These equations are then converted to a system of first order differential equations. This representation is a standard model which allows fast and modular numerical solutions to the system of differential equations [51].

2.2.1   Second order structural model – nodal model

The nodal model of a structure is a model which is based on nodal coordinates, displacements, velocities and accelerations. It incorporates mass, damping and stiffness matrices to model the structure. Also sensors and actuator locations are parts of the modeling. Let's n be the number of degrees of freedom (DOF), r be the number of outputs and s be the number of inputs. A truss structure in nodal coordinate could be modeled by the following matrix differential equations[52]:

$$M\ddot{q}(t) + D\dot{q}(t) + Kq(t) = B_0 u(t) \qquad (2.1)$$

$$y = C_a \ddot{q} \qquad (2.2)$$

Where:

q: Nodal displacement vector - $n \times 1$

$\dot{q}$: Nodal velocity vector - $n \times 1$

$\ddot{q}$: Nodal acceleration vector - $n \times 1$

u: Input vector - $s \times 1$

M: Mass matrix - $n \times n$

D: Damping matrix - $n \times n$

K: Stiffness matrix $-n \times n$

B_o: Input force matrix - $n \times s$ – it allocates the position of input excitation force

C_a: Output acceleration matrix - $r \times n$- it allocates the position of desired sensor locations

y: Output vector

2.2.2   Finite element formulation

As mentioned before, in this research work, the methodology has been implemented on truss structures. Thus the finite element model of space truss type structured haven been constructed for this purpose.   The element type is the 3D bar

element having 2 nodes and 3 translational DOFs at each node as shown in Figure 2-1. Thus the mass and stiffness matrices are 6×6 as follow:
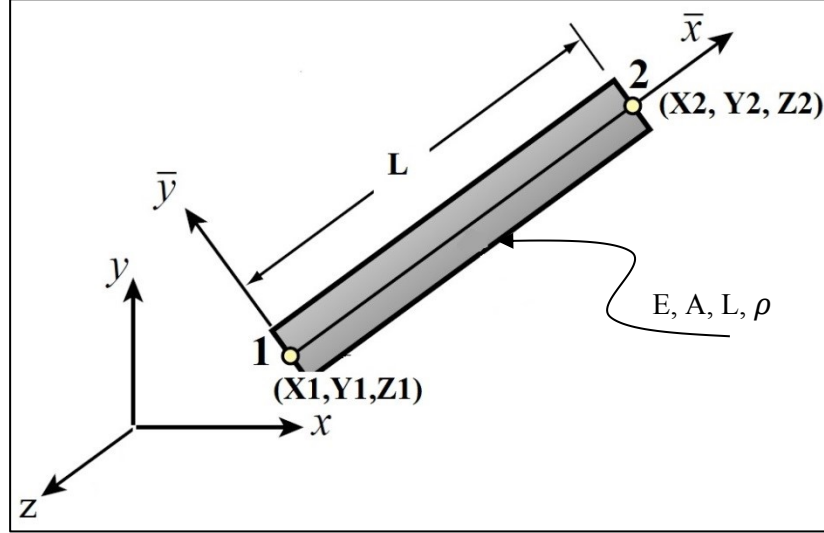
Figure 2-1: Link element for truss structure modeling

The mass matrix is considered as the lumped mass matrix. Thus it is independent of the local coordinate system.

$$M = M^{(local)} = \frac{\rho A L}{2} \begin{bmatrix} 1 & \cdots & 0 \\ \vdots & \ddots & \vdots \\ 0 & \cdots & 1 \end{bmatrix}_{6\times6} \tag{2.3}$$

where: ρ:density, A:cross section area, L: truss member length

The stiffness matrix in global coordinate can be written as [52]:

$$K = \frac{EA}{L} \begin{bmatrix} l^2 & lm & ln & -l^2 & -lm & -ln \\ lm & m^2 & mn & -lm & -m^2 & -mn \\ ln & mn & n^2 & -ln & -mn & -n^2 \\ -l^2 & -lm & -ln & l^2 & lm & ln \\ -lm & -m^2 & -mn & lm & m^2 & mn \\ -ln & -mn & -n^2 & ln & mn & n^2 \end{bmatrix}_{6\times6} \tag{2.4}$$

Where E is the modulus of elasticity and l, m and n are direction cosines defined as:

24

$$l = \frac{x_2 - x_1}{L}, \qquad m = \frac{y_2 - y_1}{L}, \qquad n = \frac{z_2 - z_1}{L}$$

2.2.3   State Space representation

State space representation incorporates only first degree differential equations. Eqs 2.1 and 2.2 could be easily rewritten in the following form:

$$\ddot{q} + M^{-1}D\dot{q} + M^{-1}Kq = M^{-1}B_0 u \tag{2.3}$$

$$y = C_a \ddot{q} \tag{2.4}$$

The state vector is defined as:

$$x = \begin{Bmatrix} x_1 \\ x_2 \end{Bmatrix} = \begin{Bmatrix} q \\ \dot{q} \end{Bmatrix} \tag{2.5}$$

In this case, Eqs. 2.3 and 2.4 could be written as:

$$\dot{x}_1 = x_2,$$

$$\dot{x}_2 = -M^{-1}K x_1 - M^{-1}D x_2 + M^{-1}B_0 u, \tag{2.6}$$

$$y = C_a (M^{-1}B_0 u - M^{-1}D x_2 - M^{-1}K x_1)$$

Eqs. 2.6 can be cast into the following form:

$$\dot{x} = Ax + Bu$$
$$\tag{2.7}$$
$$y = Cx + Hu$$

Then matrices A, B, C and H can be identified as:

$$A = \begin{bmatrix} 0|_{n \times n} & I|_{n \times n} \\ -M^{-1}K|_{n \times n} & -M^{-1}D|_{n \times n} \end{bmatrix}, \qquad B = \begin{bmatrix} 0|_{n \times s} \\ M^{-1}B_0|_{n \times s} \end{bmatrix},$$

$$C = \begin{bmatrix} -C_a M^{-1}K|_{r \times n} & -C_a M^{-1}D|_{r \times n} \end{bmatrix}, \qquad H = C_a M^{-1}B_0|_{r \times s} \tag{2.8}$$

25

In the state space representation the number of differential equations is doubled in sake of order reduction from second order to first order.

This completes the state space representation of the structural model. In the next section the force signal generation is discussed.

2.3   Generation and analysis of excitation signals

Each structural health monitoring process starts with performing some experiments that provide information about the objective of the experiment which is damage detection and localization. Within a limited time, as much information as possible should be retrieved. The quality of collected information within the operational constraints strongly is dependent to the excitation signal selection. Some of the operational constraints in each excitation experiment are [53]:

- Maximum excitation level that the structure could withstand

- Minimum power consumption

- Sensitivity of sensors to the inevitable noise content

The right hand side of Eq. 2.1 contains the term $u(t)$ which is the input force signal vector. These signals are generated by shakers (or actuators) connected to the structure at any arbitrary point.

The force signal must have some characteristics and should satisfy number of concerns:

- Generation of appropriate excitation signals to solve nonparametric and parametric system identification problems

26

- Having control over the frequency content of the excitation signals

- Generation of signals with predefined sampling frequency

- Nyquist-Shanon law and its mandates about the excitation signals

- Generation of the excitation signal with a user imposed power spectrum

To meet the above mentioned criteria first of all a Butterworth low pass noise filter as shown in Figure 2-2, is created. The Butterworth filter is designed to make a flat frequency response in the passband region (the range of frequencies that can pass through a filter without being attenuated) [54-55]. The reason that only lower frequencies are desirable, is that normally the very first truss structures natural frequencies are in the range of below 200 Hz. Therefore a low pass filter is required to simulate the excitation dynamics force in this sampling frequency.
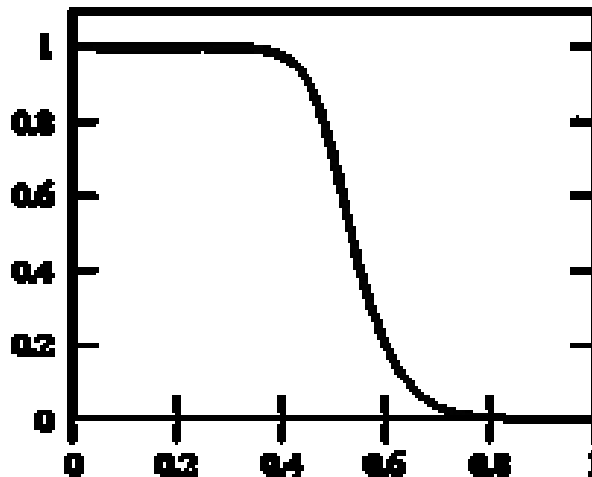
Figure 2-2: Butterworth noise filter shape with cutoff frequency of 0.4

For the 3D truss structure investigated here (Figure 2.3), the excitation force signal has a time interval of 5 seconds with 320 Hz sampling points. Hence every signal has 1600 data points. The cutoff frequency is selected to be 0.4. It means the excitation signal

has a dominant frequency content of maximum $f = 0.4 \times 320 = 128\ Hz$. This value is selected because of the nature of the 3D truss structure. This structure will be described in Chapter 3 more precisely. The first six natural frequencies of this structure are less than 128 Hz (Table 2.1), therefore this cutoff frequency is capable enough to make the signal excite the very first modes of the truss structure.
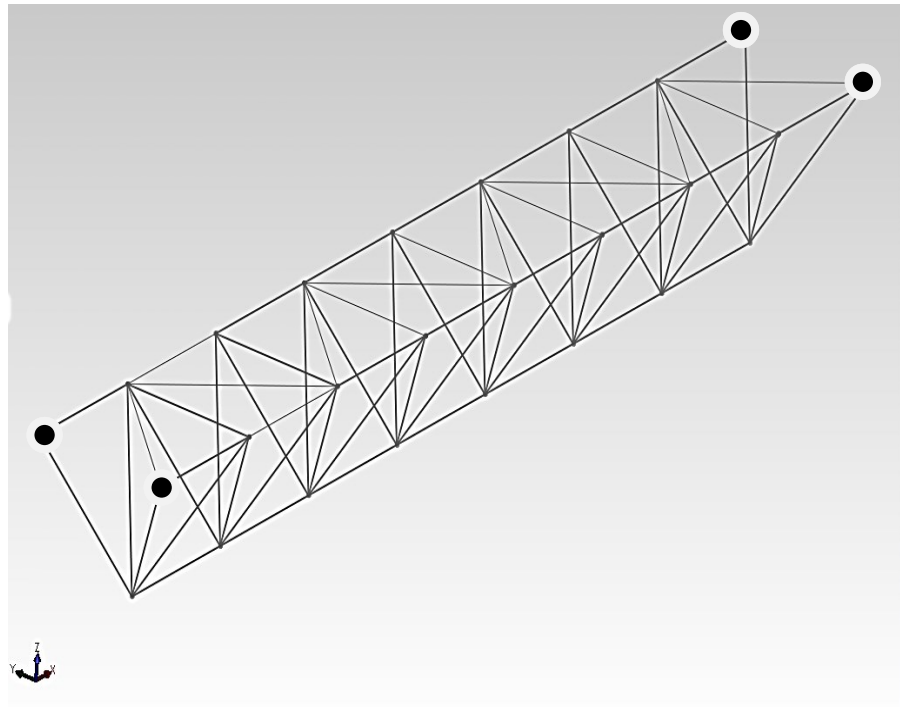
Figure 2-3: 3D truss structure fully clamped at four top nodes at left and right

Table 2.1 – First 10 modes of the 3D truss structure

	Freq. (Hz)		Freq. (Hz)
f_1	32.41	f_6	97.52
f_2	45.10	f_7	139.33
f_3	48.43	f_8	148.77
f_4	88.43	f_9	153.12
f_5	94.68	f_{10}	160.51

After selecting the cutoff frequency, time interval and number of data points (N); a random vector of size N is created. In this case $N = 5 \times 320 = 1600$. Then the Butterworth filter is applied on this vector using the `filter` command in MATLAB. The filtered vector $x(t)$ then is multiplied in a Hanning window $H(t)$ with the same time interval and data points (Figure 2.4).

$$U(t) = H(t).x(t) \tag{2.9}$$
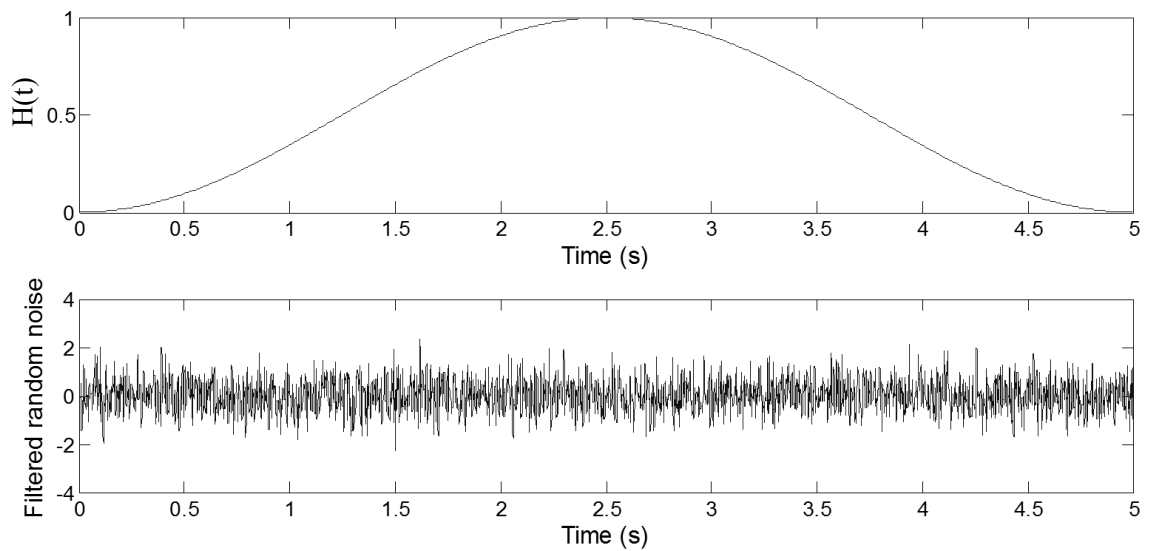
Figure 2-4: Top- Hanning window $H(t)$, down: filtered noise with sampling frequency of 320 Hz and cutoff frequency of $0.4 - x(t)$

The outcome is scaled by

$$S = \sqrt{\frac{\sum H_i^2}{N}}, \quad i = 1,2,..,N \tag{2.10}$$

$$u(t) = 100 \times \frac{U(t)}{S} \tag{2.11}$$

$u(t)$ is the filtered excitation with the user imposed power spectrum. Figure 2.5 indicates the generated signal distribution over time interval.
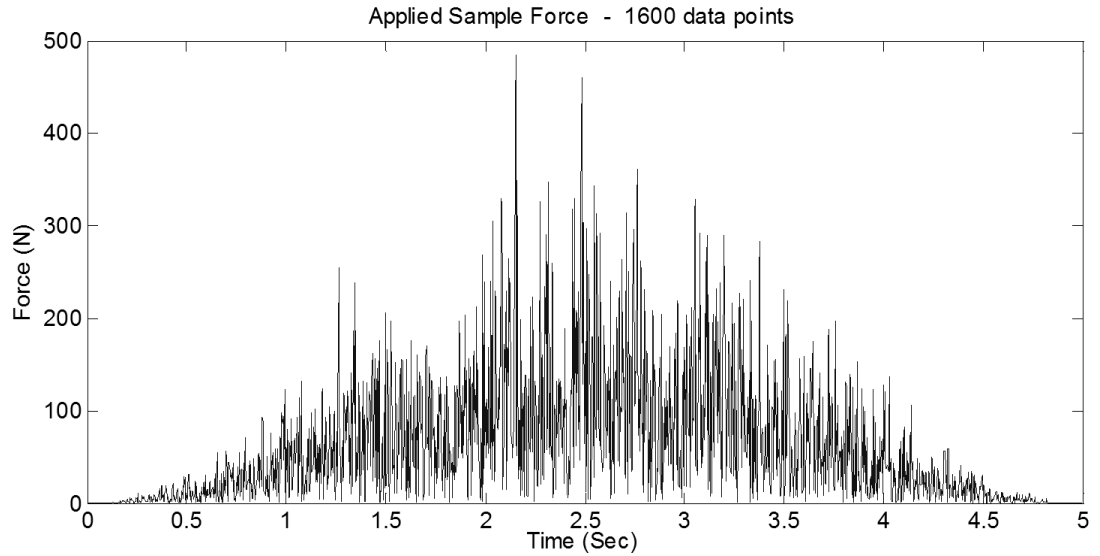
Figure 2-5: Filtered excitation signal with user imposed power spectrum – $u(t)$

The DFT (Discrete Fourier Transform) of the excitation signal and its comparison with the filter characteristics is shown in Figure 2.6. This indicates that the spectrum of filtered excitation force mainly covers the frequency contents below 128 Hz which excites the first six modes of the under study structure (Table 2-1).
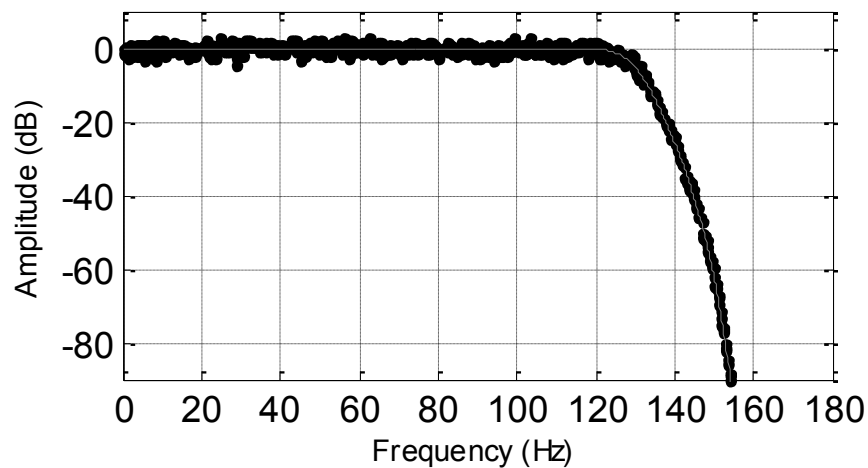
Figure 2-6: DFT spectrum of the filtered excitation force (dots) and filter characteristics (gray line) shows the good conformity of the generated signal with the ideal Butterworth lowpass filter

2.4   Frequency Response Function

Frequency Response Function (FRF) is a system characteristic which relates the output spectrum of a system to the excitation spectrum. It is used to characterize the system dynamics. It measures the magnitude and phase of the output in terms of frequency with respect to the input. For example if the system excitation signal is a sine wave with a given frequency, a linear time invariant (LTI) system will respond at the same frequency with a certain magnitude and phase angle relative to the input. It means if the input amplitude doubles the output will also double. Also for an LTI system, the frequency response is time invariant.

In structural health monitoring, this function could serve as a structure fingerprint, hence one might account it for as a damage sensitive feature. This could be realized from the fact that with similar inputs the pristine and damaged structures have different outputs. Therefore the FRFs of two structures might be a damage detection tool.

It would be possible to attach an accelerometer at a particular point on the structure and excite the structure at another point with a force actuator. Then by measuring those two signals the resulting FRF could be described as a function of frequency between those two points on the structure. The basic formula of FRF is [54]:

$$FRF\colon H(f) = \frac{Y(f)}{U(f)} \qquad\qquad (2.12)$$

Where $Y(f)$ is the sensor output and $U(f)$ is the excitation input both in frequency domain. This formula is valid when there is an explicit analytical solution between input and output.

Although the FRF is defined in Eq. (2.12) as the ratio of output and input in frequency domain, in all modern FFT analysis it is calculated in a different method as is described in Eqs. (2.13) and (2.14). The reason is to eliminate the random noise and non-linearity from the FRF estimates [56].

There are two main types of the FRF functions, $H_1(f)$ and $H_2(f)$

$$H_1(f) = \frac{Cross\ Spectral\ Density\ of\ Input\ and\ Output}{Auto\ Spectral\ Density\ of\ the\ Input} = \frac{S_{uy}(f)}{S_{uu}(f)} \qquad (2.13)$$

$$H_2(f) = \frac{Auto\ Spectral\ Density\ of\ the\ Output}{Cross\ Spectral\ Density of\ the\ Output\ and\ Input} = \frac{S_{yy}(f)}{S_{yu}(f)} \qquad (2.14)$$

Where $S_{uy}(f)$, $S_{yu}(f)$, $S_{yy}(f)$, $S_{uu}(f)$ are detailed in Eqs. (2.17) and (2.18).

$H_1(f)$ frequency response function is used in conditions where the output signal of the system is noisier than the input signal. It can be shown that H_1 is a least squared error estimate of the FRF when noise and randomly excited nonlinearity are added to the output and modeled as a Gaussian distribution [57]. This function is used in this thesis due to naturally noisier output signal than input.

Despite, $H_2(f)$ frequency response function is used in conditions where the input signal of the system is noisier than the output signal. Similarly, it can be shown that H_2 is a least squared error estimate of the FRF when noise and randomly excited nonlinearity are added to the output and modeled as a Gaussian distribution [57].

Assume the input force signal is represented by $u(t)$ and the output acceleration at a sensor location is represented by $y(t)$. Then the Fast Fourier Transform (FFT) of these two signals are:

$$Y(f) = FFT(y(t)) \tag{2.15}$$

$$U(f) = FFT(u(t)) \tag{2.16}$$

Eqs. 2.13 and 2.14 could be rewritten with more detail as:

$$H_1(f) = \frac{S_{uy}(f)}{S_{uu}(f)} = \frac{Y(f)\bar{U}(f)}{U(f)\bar{U}(f)} \tag{2.17}$$

$$H_2(f) = \frac{S_{yy}(f)}{S_{yu}(f)} = \frac{Y(f)\bar{Y}(f)}{U(f)\bar{Y}(f)} \tag{2.18}$$

Where $\bar{U}(f)$ and $\bar{Y}(f)$ are the complex conjugate of the $Y(f)$ and $U(f)$

2.5   Sensor arrangement optimization

Few literatures are available on sensor placement problem, specifically relating to SHM and damage identification. Staszewski et al. [40] studied this problem to detect and locate damage in composite materials. Shi et al. [41] investigated optimal sensor placement strategy and prioritize the sensor location according to their ability to localize structural damage based on the eigenvector sensitivity method. Gue et al. [42] also studied the global optimization using genetic algorithm technique for sensor placement. A performance function is suggested based on damage detection. Then an improved strategy for genetic algorithm is presented. The analytical results from this strategy are compared to the conventional penalty method. Finally it is concluded that the suggested method is faster and more efficient for the problem of sensor placement compare to the previous literature.

2.5.1   Problem formulation

Now let us consider the 3D truss structure shown in Figure 2.3. In this study, the optimum placement of the sensor set has been identified using the following procedure and the results are represented in Chapter 3.

To formulate this problem we introduce the continuous variable p denoting the percentage of change in stiffness and sensor placement vector M where has the cardinality of n and

$$M \subset \{1, 2, \ldots, NN\}, \quad NN = \text{number of nodes} \tag{2.19}$$

Let $\vec{u}(t)$ be the input (force) and $\vec{y}(t)$ be the output (acceleration) to a general linear time-invariant system. Also Fast Fourier Transforms of force and acceleration vectors are assumed to be $U(f)$ and $Y(f)$, respectively. As mentioned in Eq. 2.17 The output and input signals are related by the frequency response function as:

$$\text{H}(f) = \frac{S_{uy}(f)}{S_{uu}(f)} = \frac{Y(f)\overline{U}(f)}{U(f)\overline{U}(f)} \qquad (2.20)$$

The input force function is selected to be $u(t)$ as introduced in Eq. 2.11 in. The vertical accelerations are measured at all nodal points of the structure (Figure 2.3). Also it is assumed that the damage is applied on pre-known member by reducing the cross sectional area by 10% and 50% (two different cases).

Modeling of a system could be classified as either full or reduced. The full model includes measurements available at all possible DOFs and the reduced model includes only those degrees of freedom that can be measured. Obviously the reduced model is a subset of the full model.

To define the objective function $f(p, M)$, it may be the "best" sensor configuration that would minimize the difference between FRF information gathered from the full model and that gathered from the reduced model.

Let denote the system FRF at its healthy state and at each location member i by $H_i(f)$ and for the system with damaged member j the corresponding i th FRF by $H_i^j(f, p)$, for i $= 1, 2, \ldots, N$. Aggregate relative changes are then measured as sums of the relative changes in transfer function values. The full relative change $F_v(p)$ is measured as a sum over all possible output locations (full model), while the reduced

relative change $R_v\,(p, M)$ is measured as a sum over only those output locations where sensors have been placed. Thus one may write:

$$F_v(p,j) = \sum_{i=1}^{N} \left| \frac{H_i(f) - H_i^j(f,p)}{H_i(f)} \right| \qquad (2.22)$$

$$R_v(p,M,j) = \sum_{i \in M \neq \varnothing} \left| \frac{H_i(f) - H_i^j(f,p)}{H_i(f)} \right| \qquad (2.23)$$

Now the optimization problem is defined as:

$$Minimize\ f^{\,j}(p,M) = \left\| \frac{F_v(p,j) - R_v(p,M,j)}{F_v(p,j)} \right\|$$

$$(2.23)$$

$$Subject\,to : M \subset \{1,2,...,N\,N\}, \quad 0 \leq p \leq 1$$

In summary the purpose of this optimization problem is to find the nearest summation of FRF function changes of reduced model to the full model. The reduced model is a model that incorporates the limited sensor locations. This will ensure that the reduced model captures the most physical information of the structure as possible.

2.5.2   Discrete neighbor sets

For Mixed Variable Pattern Search (MVPS) problems, finding a minimizer is usually a difficult and complicated procedure, because there are many possible combinations to be considered. On the other hand, since the problem is discrete, and design variables are not continuous but bounded, the well-known gradient based optimization methods cannot be used.   Also the concept of local minimum may be confusing in this category of problems because the design variables do not have an

inherent natural ordering [46]. To define exactly what a local minimum is, first we have to define the concept of neighborhood. Assume that M is a set of n sensors and $M \subset \{1, 2, ..., NN\}$, where NN is the number of nodes.

Set N is called a neighbor-1 of M if it has the same cardinality of n and only one of its members is a single unit more or less of one of the members of M and all members of N are distinct and less than or equal to the upper bound or greater than or equal to the lower bound. For example if $M = \{2, 5, 7, 8\}$ the sets of neighbors will be:

$$N_1 = \{3, 5, 7, 8\}, \ N_2 = \{1, 5, 7, 8\}, \ N_3 = \{2, 4, 7, 8\}, \ N_4 = \{2, 6, 7, 8\}$$

$$N_5 = \{2, 5, 6, 8\}, \ N_6 = \{2, 5, 7, 9\}$$

Neighbor-Δ, means one element of N_i differs from one of the elements in M, by Δ

Definition: Point $x = (p, M) \in X$ is a local minimizer of f with respect to the set of neighbors $\mathcal{N}(x) \subset X$ if there is an $\epsilon > 0$ such that $f(x) \leq f(v)$ for all v in the set.

$$X \cap (\cup_{y \in \mathcal{N}(x)}(B(y^c, \epsilon) \times \{y^c\}) \tag{2.24}$$

Where, $B(y^c, \epsilon)$ is an open ball of radius $\epsilon > 0$ of y^c centered neighborhood. Also this set accounts for discrete neighbors of x [46].

2.5.3 MVPS algorithm

To find the optimum sensor arrangement the following algorithm has been presented:

1) Let $x_0 \in X$ satisfy $f_X(x_0) < \infty$ and choose a tolerance ξ (termination criteria)

2) Set $\Delta_0 = 1$

3) For $k = 0,1,2, ...,$ do the following

4) Search step: Employ some finite strategy seeking an improved mesh point;

   i.e., $x_{k+1} \in M_k$ where $f_X(x_{k+1}) < f_X(x_k)$. (In this case we may compare the objective function for all sets of neighbors and select the minimum).

5) Extended search step: If the search step did not find a better result among neighbor set, then extend the neighbor-Δ_0 set to $\Delta_0 = \Delta_0 + 1$ and search again until an improved mesh point is found or until all points are exhausted.

6) Update: If search or extended search step finds an improved mesh point, update x_{k+1}

7) If $|f_X(x_{k+1}) - f_X(x_k)| < \xi$ STOP otherwise go to step 2.

In Chapter 3 the truss structure represented in Figure 2-3 is studied and the optimum sensor arrangement to detect the damage at specific location is found.

2.6 Damage sensitive feature extraction: statistical approach

In the SHM field of study it is essential to find damage sensitive features which can distinguish between healthy and damaged states. Preferably these features should not be sensitive to operational or environmental conditions. However this cannot be met in most real situations[58-59]. In this section some statistical based feature extraction techniques are introduced.

Basic statistical properties of calculated time history data are also presented. The first four statistical moments as well as autoregressive parameters are part of feature extraction procedure. These features later are used to cluster and classify different time history signals.
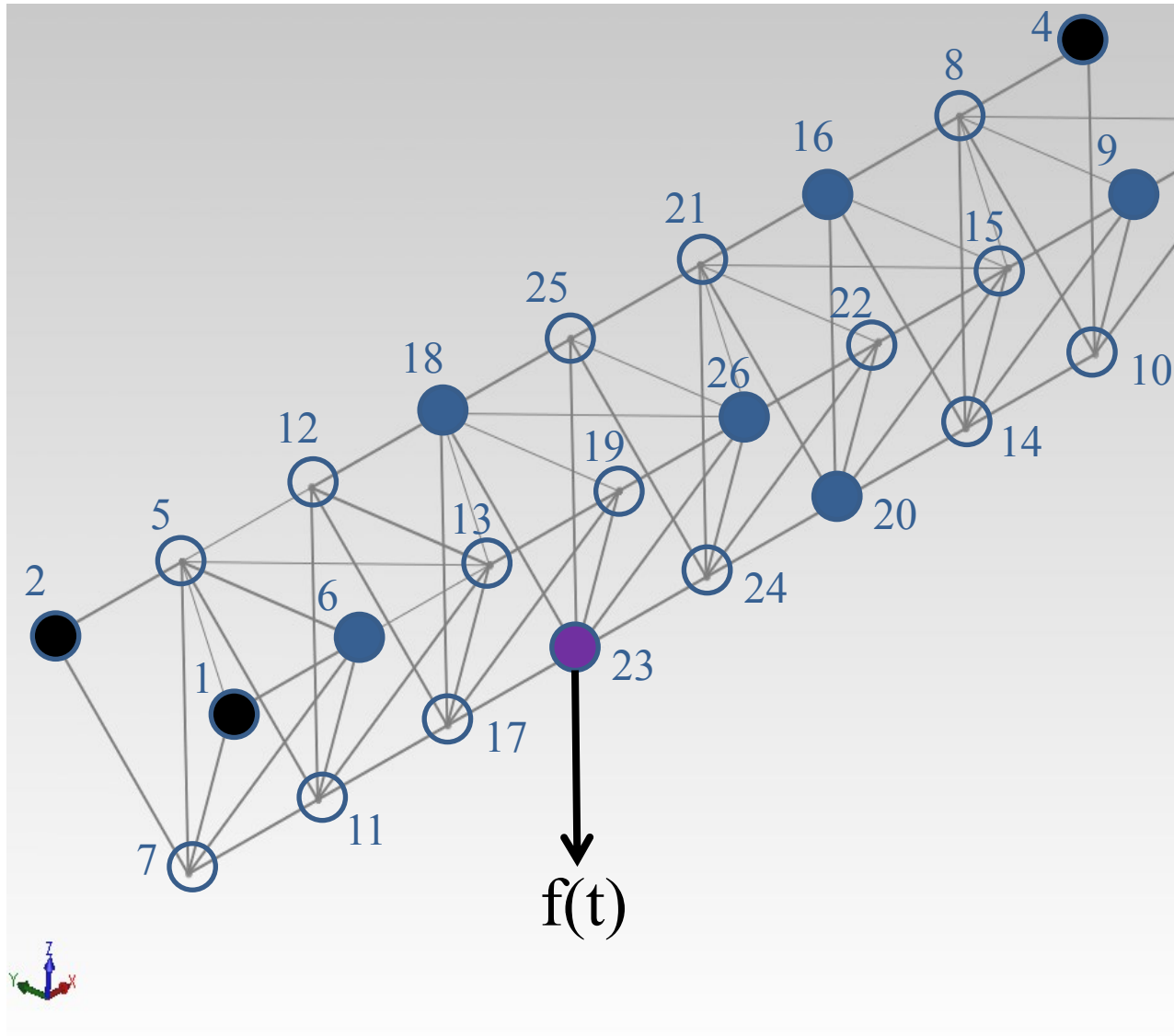
Figure 2-7: Truss structure clamped at nodes 1 to 4, excited at node 23 and sensor locations at nodes {6, 9, 16, 18, 20, 26}

Assume the 3D truss structure shown in Figure 2-7 is excited by the external force at node 23. The horizontal and vertical distance of each node from its nearest adjacent node is 1 meter. The cross section of each member is a solid square $50mm \times 50mm$. The accelerometers are situated at six different nodes {6, 9, 16, 18, 20, 26} which are

distinguished from other nodes in Figure 2-7. Figure 2-8 shows sample signals from these sensor locations for healthy structure case:
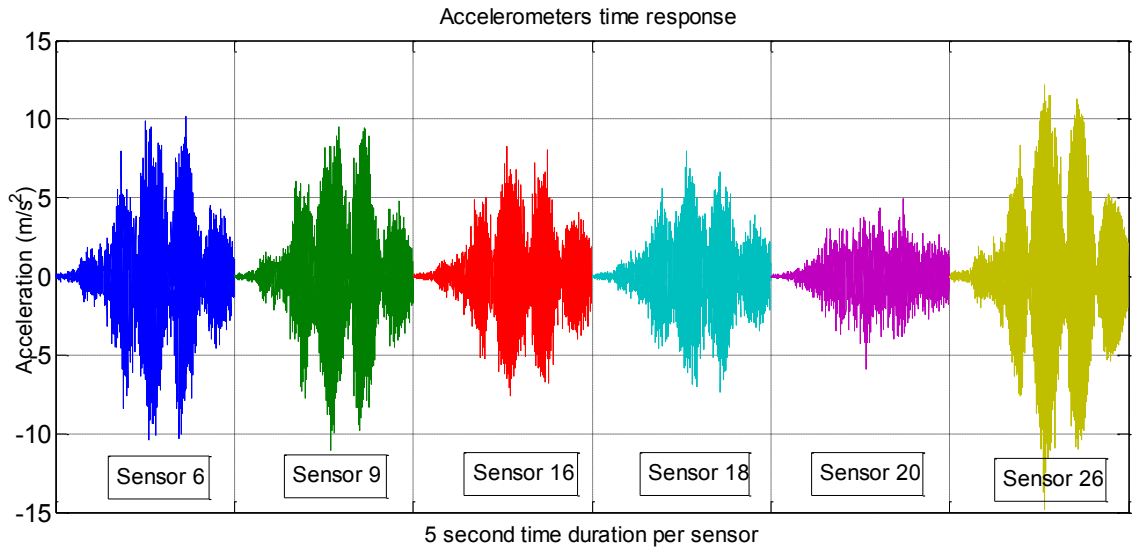
Figure 2-8: Time response for healthy structure
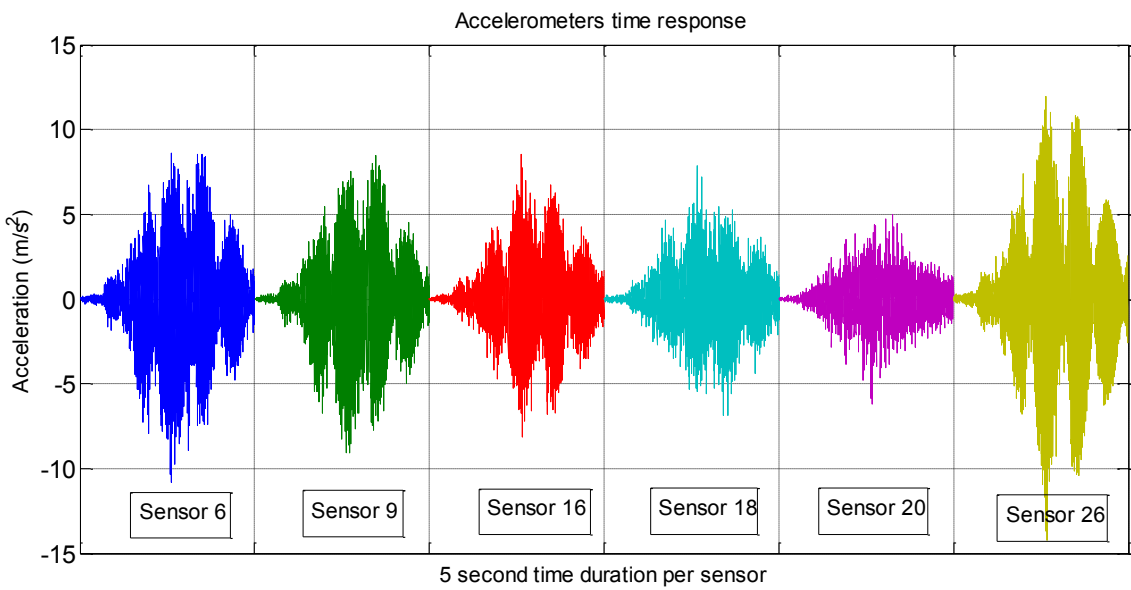
Figure 2-9: Time response for damaged structure – 30% cross section reduction in member
connecting nodes13 and19

Now, the damage has been introduced by cross section reduction in one specific

member. For instance if the member connecting nodes 13 and 19 is cracked and the crack

size is 15 mm, then the reduction in the cross-section of this member can be calculated as

(original cross section was 50 mm x 50 mm):

$$Area\ reduction\% \ = \frac{A^{healthy} - A^{damaged}}{A^{healthy}} \times 100 = 30\% \qquad (2.25)$$

Figure 2-9 indicates the sensor acceleration outputs for described damaged case to

the force input on node 23. It should be noted that for the damaged case, the applied

dynamic force is the same as that for the healthy case plus a small white noise.

Figure 2-10 indicates the applied forces for two different cases. The signal to noise ratio

(SNR) is assumed to be 20.
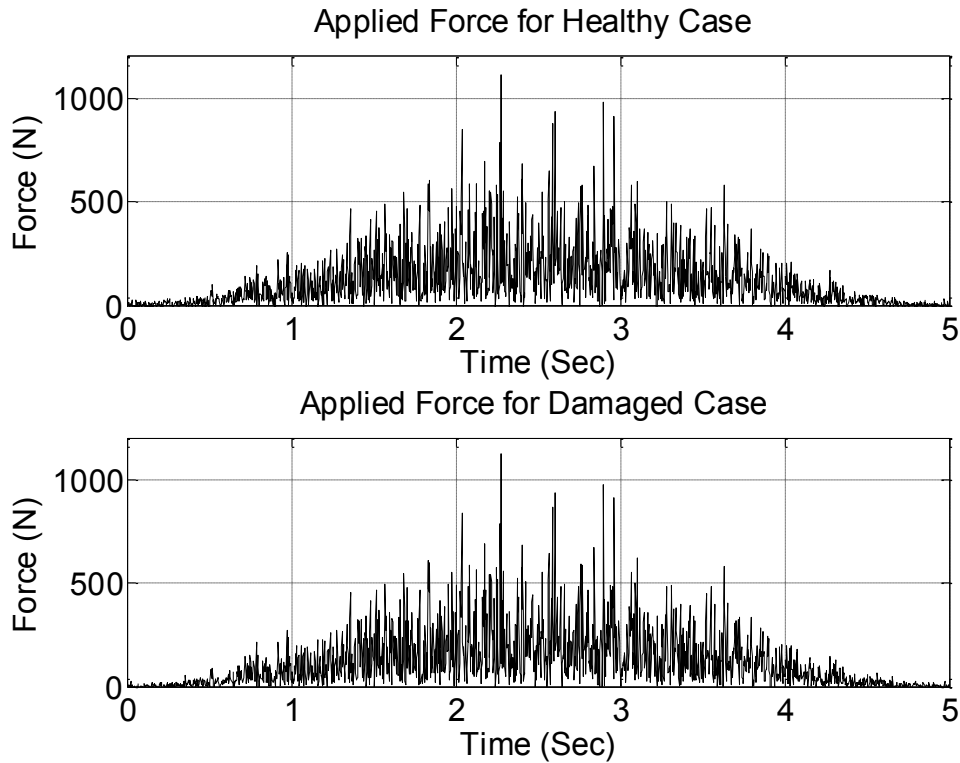
Figure 2-10: Applied force for two cases: healthy and damaged with added noise with SNR=20

To introduce the damage sensitive feature 10 different cases including 5 healthy and 5 damaged cases were studied. The difference among healthy cases is the applied force which has some added noise to a baseline force signal. This assumption is realistic because while doing the experiment, noises are always there and no two actuator output signals in different times are exactly the same.

Case 1: Healthy state

Case 2: Healthy state

Case 3: Healthy state

Case 4: Healthy state

Case 5: Healthy state

Case 6: Damaged state - damaged member DM = 1 (Nodes 13-19)

Case 7: Damaged state - damaged member DM = 2 (Nodes 21-25)

Case 8: Damaged state - damaged member DM = 3 (Nodes 15-16)

Case 9: Damaged state - damaged member DM = 4 (Nodes 22-24)

Case 10: Damaged state - damaged member DM = 5 (Nodes 12-17)

The damage locations and their corresponding case number are clearly shown in Figure 2-11.
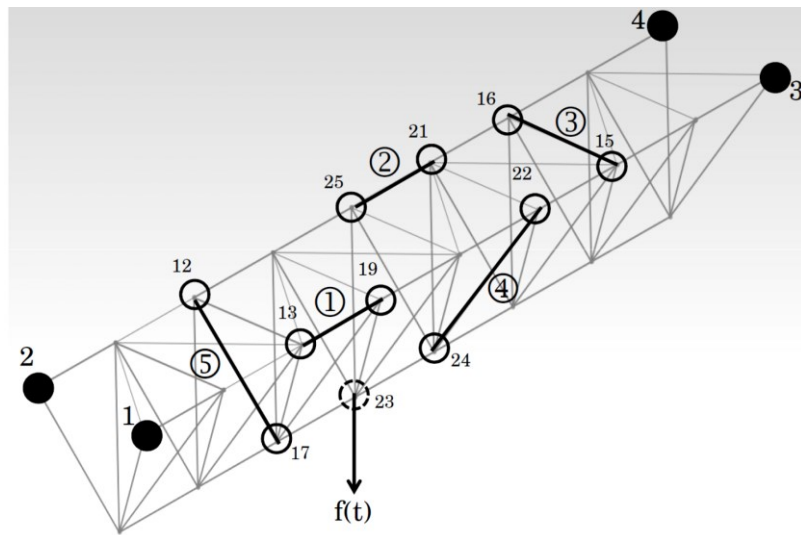
Figure 2-11: Damage locations and their corresponding case number

2.6.1 Statistical moments

The statistical moments (mean, variance, skewness, and kurtosis) are often used to process raw time-series data. Also statistical moments can serve as damage sensitive features, as it can be seen from Figure 2-12, these moments are sensitive to damage and show some deviation from the trend of healthy cases.

The first raw moment is the mean of data, and describes the tendency of data about its mean value.

$$\mu_X = E(X) = \frac{1}{n}\sum_{i=1}^{n}x_i, \quad X = \{x_1, x_2, ..., x_n\} \tag{2.26}$$

$E(X)$ is also called the mathematical expectation.

Usually, the data vector is centralized by reducing its mean value from each vector component. Thus the first moment of centralized data is always zero. In other words,

$$\mu_1 = E(X - \mu_X) = \frac{1}{n}\sum_{i=1}^{n}(x_i - \mu_X) = 0 \tag{2.27}$$

The second raw moment is the variance and is the square of standard deviation. It is defined as:

$$\sigma_X^2 = E(X - \mu_X)^2 = \frac{1}{n-1}\sum_{i=1}^{n}(x_i - \mu_X)^2 \tag{2.28}$$

The standard deviation σ_X indicates the spread of data about the mean.

The third raw moment is called the skewness and is defined as:

$$S = \frac{E(X - \mu_X)^3}{\sigma_X^3} \tag{2.29}$$

Positive skewness means that the right tail in the data distribution bell type diagram is longer and that the area of the distribution is concentrated below the mean. On the other hand, a negative skewness means that the left tail is longer and that the area of the distribution is concentrated above the mean. The skewness of a standard normal distribution is zero [58, 60].

The fourth statistical moment is a measure of the relative amount of data located in the tails of a probability distribution. The kurtosis, k, is the normalized fourth statistical moment and is defined as:

$$k = \frac{E(X - \mu_X)^4}{\sigma_X^4} \qquad (2.30)$$

Kurtosis greater than 3 indicates more data far from the mean and is common to "peaked" type data distribution. If the kurtosis is less than 3, the data distribution is flat with short tails. The kurtosis of standard normal distribution is exactly equal to 3 [60].

Figure 2-12 indicates the first four moments of data obtained from the sensors in Figure 2-7 for above-mentioned cases.
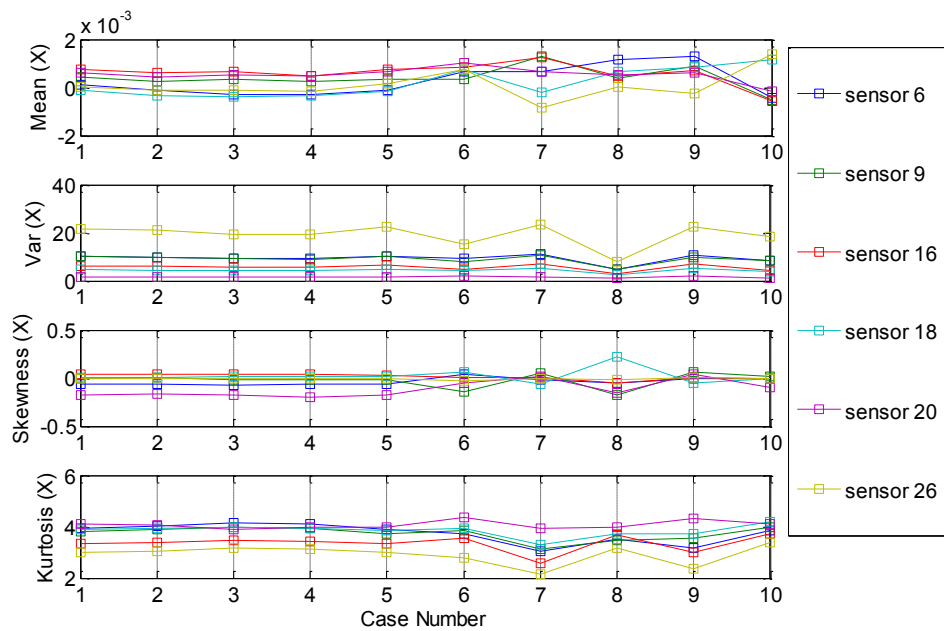
Figure 2-12: First four statistical moments for 10 different cases and 6 sensor data set

As it can be realized, healthy cases 1-5 are following almost steady flat lines while the damaged cases are evidently deviated from the straight lines, so these moments are sensitive to damage. There are other sensitive features like the wavelet coefficients, FRF, and autoregressive parameters. In the next section the autoregressive parameter of a signal is discussed.

2.6.2 Autoregressive parameters

Data points in the time series may have an internal structure like autocorrelation, trend or seasonal variation [58]. Autoregressive (AR) parameters are a tool which could reveal these correlations and connections. They can reduce the large cardinality of the time responses to manageable and interpretable data sets. With the aid of autoregressive parameters one can distinguish between healthy and damaged cases.

The AR parameters with order p satisfy the following equation:

$$x_i = \sum_{j=1}^{p} \phi_j x_{i-j} + \varepsilon_i, \ i = 1,...,n \tag{2.31}$$

In equation 2.31, x_i is the ith term in the time series $X(t)$ and ε_i is the error. The AR parameters ϕ_j can calculate the nth term of a time series by the weighted summation of its last p terms with an error of ε_i. The unknown parameters ϕ_j can be calculated using two approaches. First one is the least square method (linear regression) and the second one is the Yule-Walker equation [61-63]. In this thesis the former is used and expanded due to its simplicity and acceptable performance.

2.6.3 Least square method to estimate AR parameters

In this section the application of least square method to estimate AR parameters is briefly explained. Given a data set $\left\{ y_i, x_{i1},...,x_{ip} \right\}, i = 1,...,n$ where dependent variable y_i and $p-vector$ of regressors or predictor variables x_i have a linear relationship. It means

$$y_i = \phi_1 x_{i1} + ... + \phi_p x_{ip} + \varepsilon_i = \mathbf{X_i^T} \boldsymbol{\varphi} + \varepsilon_i, \ i = 1,...,n \tag{2.32}$$

These n equations are stacked together and written in vector form as:

$$\mathbf{y} = \mathbf{X}\boldsymbol{\varphi} + \boldsymbol{\varepsilon} \tag{2.33}$$

where

$$\mathbf{y} = \begin{pmatrix} y_1 \\ y_2 \\ \vdots \\ y_n \end{pmatrix} \quad \mathbf{X} = \begin{pmatrix} \mathbf{X_1^T} \\ \mathbf{X_2^T} \\ \vdots \\ \mathbf{X_n^T} \end{pmatrix} = \begin{pmatrix} x_{11} & x_{12} & \cdots \\ x_{21} & x_{22} & \cdots \\ \vdots & & \\ x_{n1} & x_{n2} & \cdots \end{pmatrix} \quad \boldsymbol{\varphi} = \begin{pmatrix} \phi_1 \\ \phi_2 \\ \vdots \\ \phi_n \end{pmatrix} \quad \boldsymbol{\varepsilon} = \begin{pmatrix} \varepsilon_1 \\ \varepsilon_2 \\ \vdots \\ \varepsilon_n \end{pmatrix} \quad (2.34)$$

Neglecting the error, the AR parameters can be found as:

$$\boldsymbol{\varphi} = (X^T X)^{-1} X^T \mathbf{y} \qquad (2.35)$$

2.6.4 AR model order

The AR model order is not a known value. A high-order model matches the data perfectly, but when it comes to other data sets, it cannot be used with great sensitivity to damage. Also, a low-order model will not capture the physical system response precisely.

There are several techniques in the literature to find out the optimum model order, such as Akaike's Information Criterion (AIC), Partial Autocorrelation Function (PAF), Root Mean Squared Error (RMSE) and Single Value Decomposition (SVD). These techniques suggest an optimum AR model order between 10 to 30 [58]. In this study the AR model order of 20 is used.
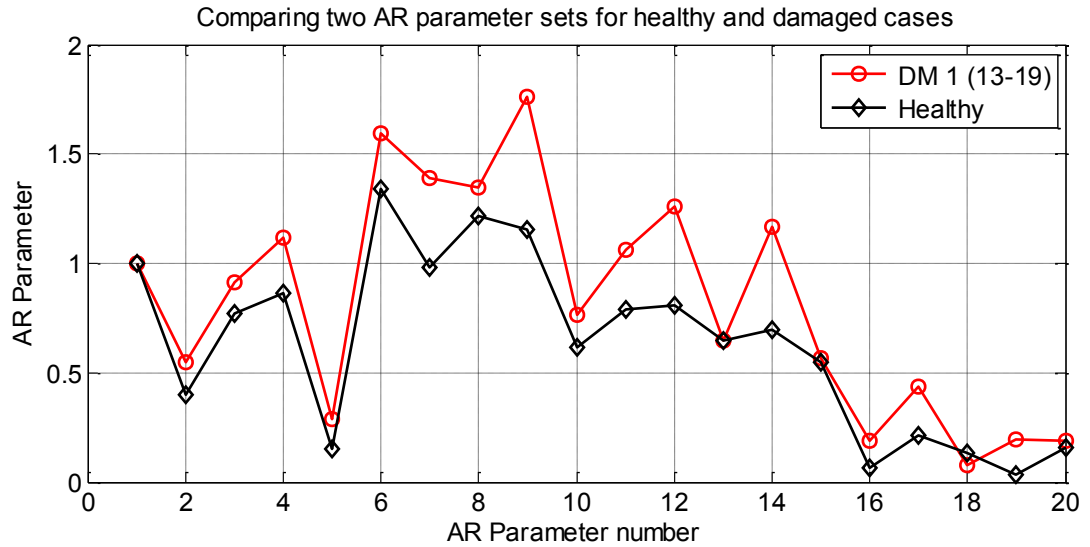
Figure 2-13: AR parameters of two different cases: healthy and damaged in member 1 connecting nodes 13 and 19 using the sensor at node #6 data

Figure 2-13 indicates the comparison between two healthy and damaged cases and the high sensitivity of the AR parameters to damage is clear, using the obtained data from sensor at node 6. The AR parameter order is assumed to be 20. After studying this figure, one may find out that the AR parameters of the damaged case are completely distinguishable from the healthy case. This is a great finding that helps to detect the damaged cases from the healthy ones.

Figure 2-14 shows two healthy cases with slightly different loading condition with added noise. It is clear that these two cases are almost identical. Comparing Figures 2-13 and 2-14 clearly indicates the sensitivity of the AR parameters to slight damages in the structure.
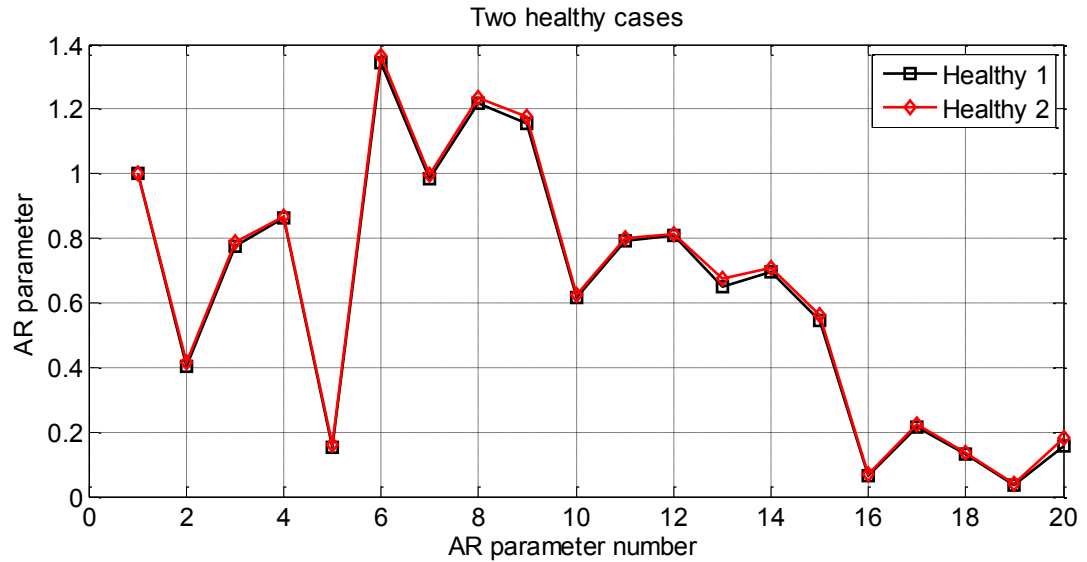
Figure 2-14: AR parameter for two healthy cases, obtained from sensor at #6

2.7 Damage Index and data clustering

In structural health monitoring two aspects are very important, damage detection and damage localization. These are actually the first two steps of a complete SHM package. The other two aspects are damage sizing and estimating the remaining life and finally the prognosis (Figure 1-1).

In this section the damage detection procedure for a truss structure has been studied and a Damage Index (DI) has been introduced. In the previous section it is found that the AR parameters are very sensitive to the damage, hence one may effectively utilize the AR parameters to categorize the output signals into healthy or damaged state based on the previously established knowledge.

In order to detect the damage a baseline data is essential. As mentioned before, in this study 5 realizations of healthy state with slightly different input force is employed to create a baseline reference data.

Figures 2-15 to 2-20 show the extracted AR parameters for 5 healthy and 5 damaged cases. Each Figure corresponds to one installed sensor and the extracted AR parameters. The AR model order is selected to be 20 based on the discussions in the 2.6.4. These figures show that the AR parameters of damaged cases deviate big enough from the healthy cases. This proves them very sensitive to detect damage in truss structures.

It should be noted that there are 20 AR parameters per sensor and thus for 6 sensors, in total, there are120 parameters for each case. These 120 AR parameters will further be used as feature vector to be fed into the SVM tool.

Figure 2-15: AR parameters for sensor #6, and for healthy and different damaged cases
H: Healthy, D: Damaged

Figure 2-16: AR parameters for sensor #9, and for healthy and different damaged cases
H: Healthy, D: Damaged

Figure 2-17: AR parameters for sensor #16, and for healthy and different damaged cases
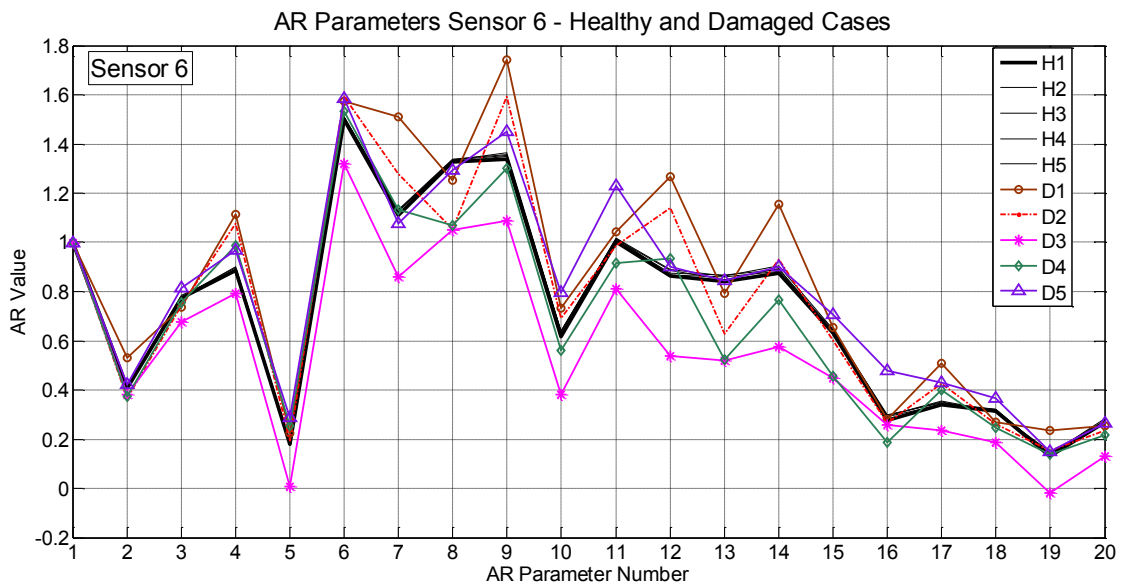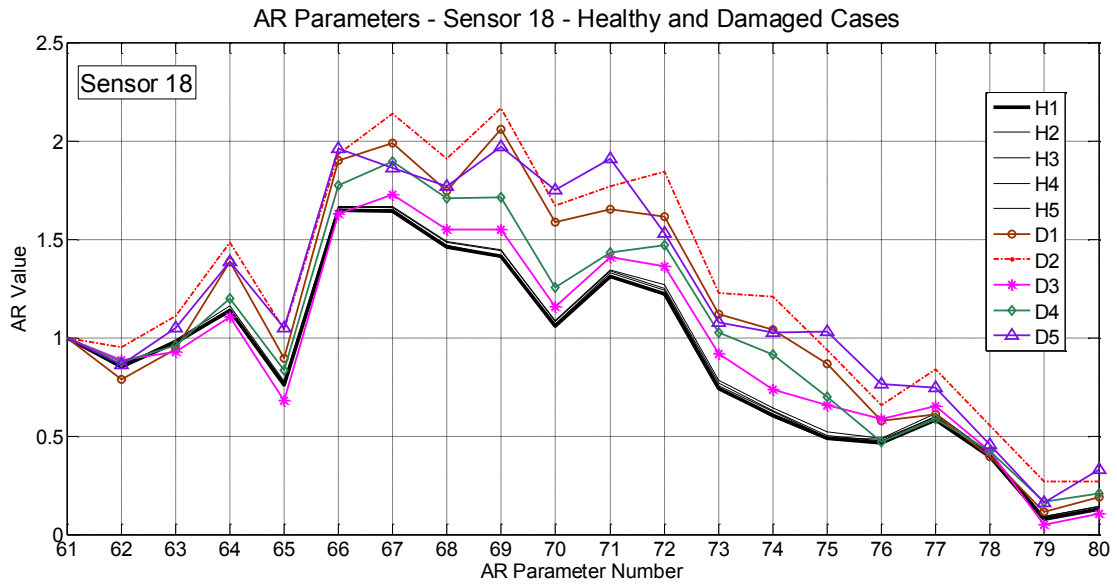
Figure 2-18: AR parameters for sensor #18, and for healthy and different damaged cases
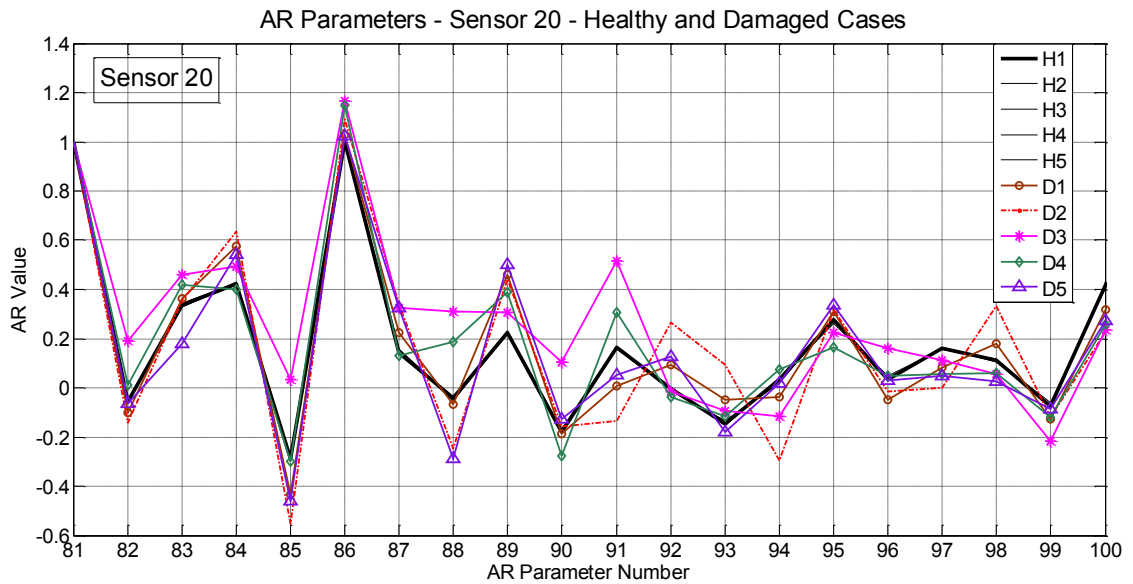
H: Healthy, D: Damaged

Figure 2-19: AR parameters for sensor #20, and for healthy and different damaged cases
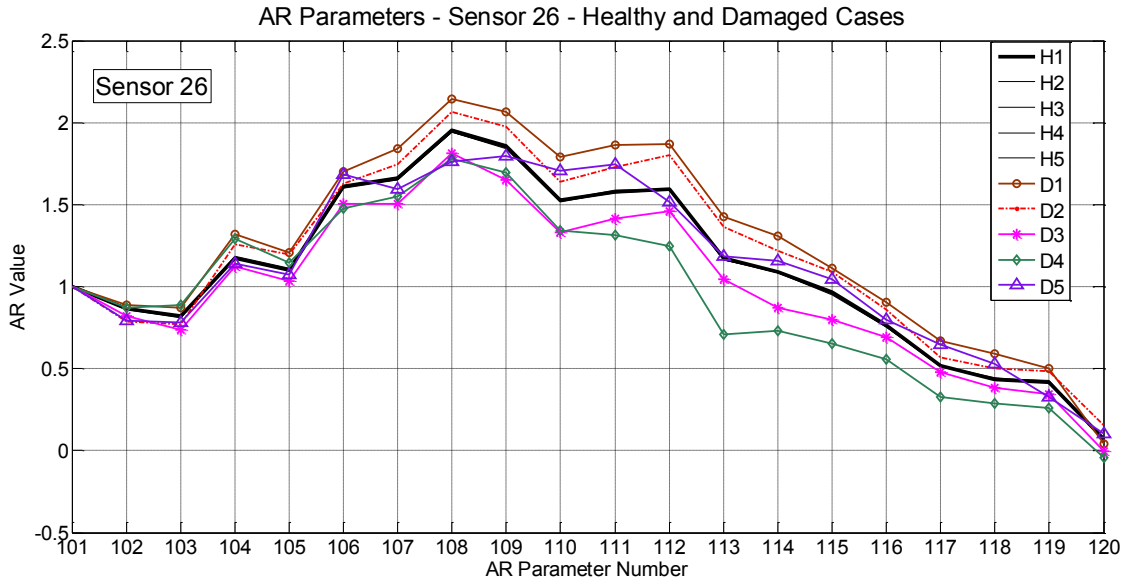
H: Healthy, D: Damaged

Figure 2-20: AR parameters for sensor #26, and for healthy and different damaged cases

H: Healthy, D: Damaged

From close examination of Figures 2-15 to 2-20, one may find that the standard deviation from the baseline reference data could be an indicator of structural state. The baseline reference data is chosen to be the average of autoregressive parameters of at least five healthy states.

$$BaseLine\ Data = \frac{1}{NR} \sum_{i=1}^{NR} AR_i^{healthy}$$ (2.36)

Where

$$NR = \max(\#\ of\ healthy\ state\ realization, 5)$$ (2.37)

The damage index is chosen to be the standard deviation of AR parameters of each signal from the baseline data

$$DI = \text{std}(AR^{unknown\,state} - BaseLine) \qquad\qquad (2.38)$$

A threshold is also required to separate the damaged and healthy states, In other words, if the DI of an unknown state is above the threshold value, it indicates a damaged state. Here in this study, the threshold value is defined as:

$$Threshold = 2 \times \frac{1}{NR} \sum_{i=1}^{NR} DI_i^{healthy} \qquad\qquad (2.39)$$

The multiplier 2 in Eq. 2.39 is selected based on try and error. The threshold line which is built based on this multiplier can distinguish the damaged and healthy cases in most of the times. Further explanation will be done in sensitivity analysis section in Chapter 3. This is one of the most significant contributions of the present thesis that is found by the author.

Figure 2-21 illustrates the DI based on sensor #6 for 10 different cases (5 healthy and 5 damaged) and the threshold line. As it can be realized the damaged index based on the AR parameters enable to accurately identify all damaged cases.
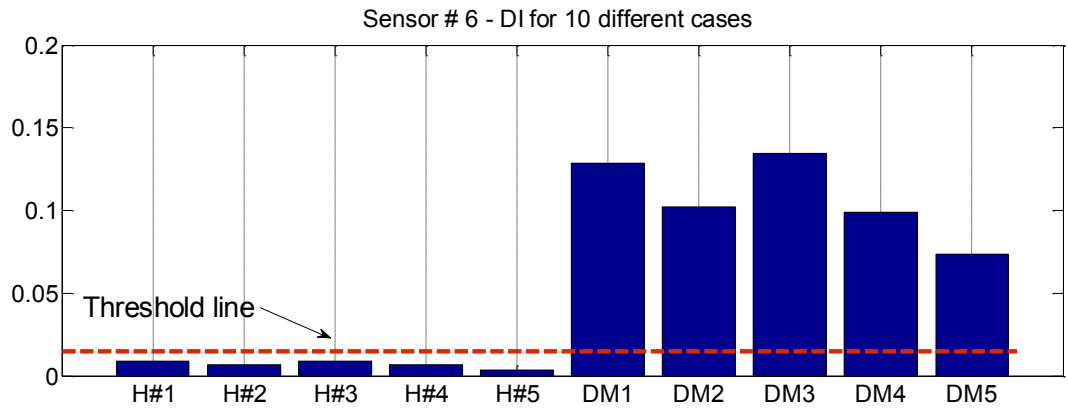
Figure 2-21: Damage Index (DI) obtained from sensor #6 and data clustering (damage detection)

Utilizing other sensors will also provide the same information and can accurately identify the damaged cases. More detail will be prepared in the next Chapter on this topic.

This completes the damage detection phase which only requires one sensor data. In the next section, the damage localization technique using the support vector machine (SVM) tool is introduced.

2.8   Damage localization

2.8.1   Feature vector classification

This section introduces a new approach to damage localization and feature classification, assuming that damage has already been determined to be present and that there is only one occurrence of damage in the whole structure. This statistical based approach relies on the accurate modeling of the structure and consequently, the presence of a rich data base of all possible damage locations and structural response to slightly different loading conditions. To accomplish the localization task, "enough" number of realizations should be generated and stored in data matrices. Normally 10 realizations (based on try and error) per case with slightly different loading conditions are enough. A feature vector is generated per every realization and all together ensembles to a feature matrix. This feature matrix is then fed to a training procedure to create a *trained model*.

After building the trained model, a sample test data is generated and based on the trained model, the corresponding category of each sample data is predicted. Usually the sample data is just one realization of all damaged cases to check the accuracy of the trained model. The accuracy in prediction depends on few factors like the severity of

damage, feature vector (AR parameters) length, number of sensors and applied force location.

2.8.2 Support Vector Machine

Support Vector Machine (SVM), is the main tool to categorize feature vector data and build the trained model. SVM is a powerful tool which its basic idea was initiated in 1979 by Vapnik [64] and developed by himself in 90's [65-66].

SVM is a pattern recognition and data categorization tool which separates data points with maximum correlation and put them together in one category. The correlation among the data inside each category is maximized while the correlation among different categories is minimized.
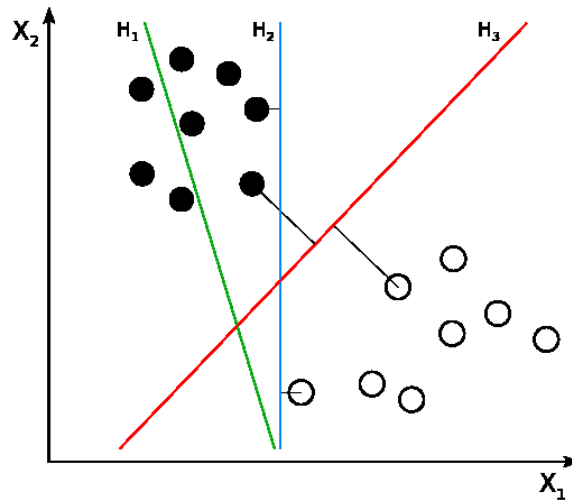
Figure 2-22: H_1 (green) does not separate the classes. H_2 (blue) does, but only with a small margin. H_3(red) separates them with the maximum margin [67]

Figure 2-22 shows the main idea of linear SVM in 2D in which the SVM algorithm finds the line with the greatest possible margin (red line) as the separator of two categories of data which are black dots and white dots.

Sometimes the data cannot be separated linearly and a nonlinear classifier is required to categorize the data. In these cases a kernel function is applied [68]. Figure (2-18) gives the main idea of the nonlinear SVM. In nonlinear SVM kernel function $x \rightarrow \varphi(x)$ maps the data set to a space (for example a spherical surface) which a linear hyperplane is able to categorize data with maximum correlation.
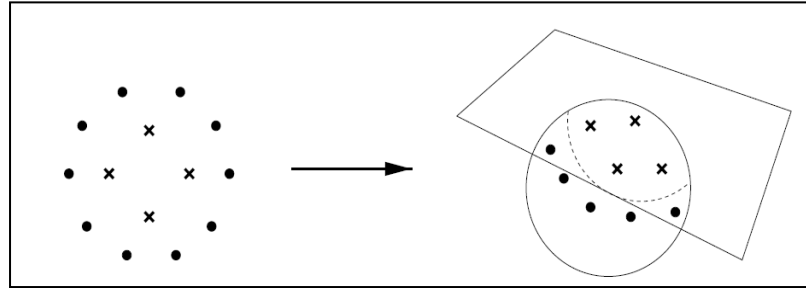
Figure 2-23: Data set that cannot be separated linearly (left), a linear hyper plane that separates data by using a kernel function

In the truss structure which is discussed previously, the Damage Sensitive Features (DSFs) are AR parameters. Unlike the damage detection, to localize the damage all information from all sensors is required. DSFs are assembled into one big matrix namely Damage Sensitive Matrix (DSM).

$$DSM^{(i)} = \begin{bmatrix} DSF_1^T \\ DSF_2^T \\ \vdots \\ DSF_6^T \end{bmatrix}^{(i)} = \begin{bmatrix} AR_{1,1} & AR_{1,2} & . & . & . & AR_{1,6} \\ AR_{2,1} & AR_{2,2} & . & . & . & AR_{2,6} \\ . & . & . & & & . \\ . & . & . & . & & . \\ . & . & & . & . \\ AR_{20,1} & AR_{20,2} & . & . & . & AR_{20,6} \end{bmatrix}^{(i)} , \quad i = 1,2,...,NR \qquad (2.40)$$

Where each column of the DSM matrix is a feature vector corresponding to a sensor which is numbered by the column number. The number of columns is equal to the number of installed sensors and NR is the number of realization. The assembled DSM

matrix which includes all realizations is called the training set which must be prepared in a special format. This format will be elaborated with more details in the next chapter.

When the training procedure is accomplished, and the predictor model is completed; a set of test data is generated and is introduced to develop the trained model. The SVM based trained model categorizes these data and predicts which signal is representing.

Here, a SVM software named LibSVM [69] has been used to develop the trained model. LibSVM is an integrated software for support vector classification, regression and distribution estimation [70].

CHAPTER 3

SIMULATION RESULTS AND DISCUSSION

3.1 Introduction

The theory and formulation of the SHM package is elaborated in Chapter 2. In this Chapter the application of those theories is performed on a sample truss structure. A truss structure is modeled, validated and the suggested SHM package is applied to show the capability of the approach. The model is validated by making a comparison between ANSYS® results and the developed FE code in MATLAB® environment.

3.2 Truss structure designation

Figure 3-1 indicates the studied space truss structure which has 70 members of uniform cross section. The cross sections are all solid square and the joints are hinged in all directions by spherical joints. The far most left and right top nodes are fully constrained in all directions. Dynamic force is applied on node C and is indicated by $F(t)$. Dimensions are shown clearly in Figure 3-1.
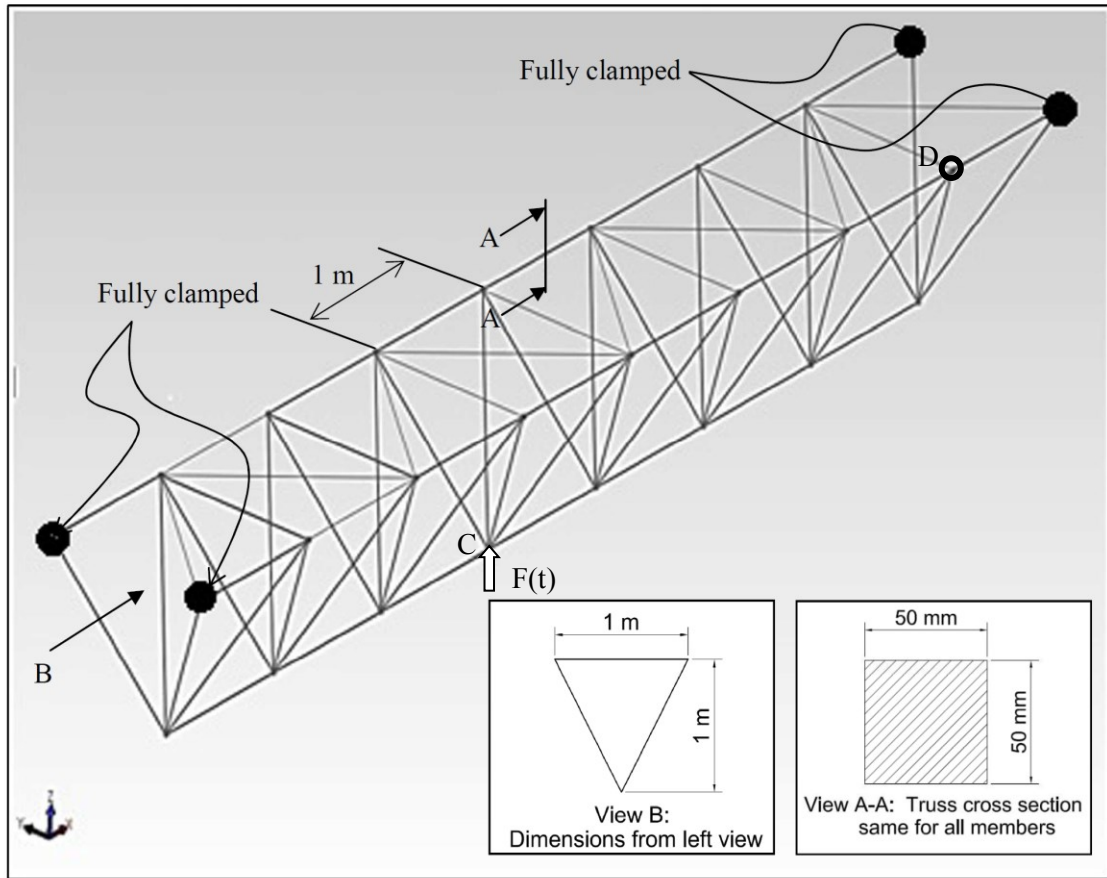
Figure 3-1: Truss structure designation, dimensions, and loading condition

3.3 Model validation

To model the truss structure, finite element analysis is employed and by state space representation, the system of first order differential equations are built and solved. The time response of each node of the system under dynamic loading condition is obtained. A number of sensors are installed exactly on selected nodes. The sensor responses are the acceleration responses at sensor locations.

The developed FE model in MTALB has been validated using ANSYS. The results for the first 10 natural frequencies obtained from MATLAB and ANSYS are provided in Table 3-1.

Table 3-1: Comparison between first 10 natural frequencies of MATLAB and ANSYS built models

	MATLAB Freq. (Hz)	ANSYS Freq. (Hz)		MATLAB Freq. (Hz)	ANSYS Freq. (Hz)
f_1	32.41	32.41	f_6	97.52	97.52
f_2	45.10	45.10	f_7	139.33	139.33
f_3	48.43	48.43	f_8	148.77	148.77
f_4	88.43	88.43	f_9	153.12	153.12
f_5	94.68	94.68	f_{10}	160.51	160.51

Apparently, the results from MATLAB and ANSYS are exactly the same even with more than two decimal points. This validates the FEM formulation that is developed in the MATLAB program.

To validate the dynamic time response, an impulse force is applied on the node C (Figure 3-1) and the acceleration of a selected node D is calculated over a time period of 5 seconds. The impulse force diagram is shown in Figure 3-2.
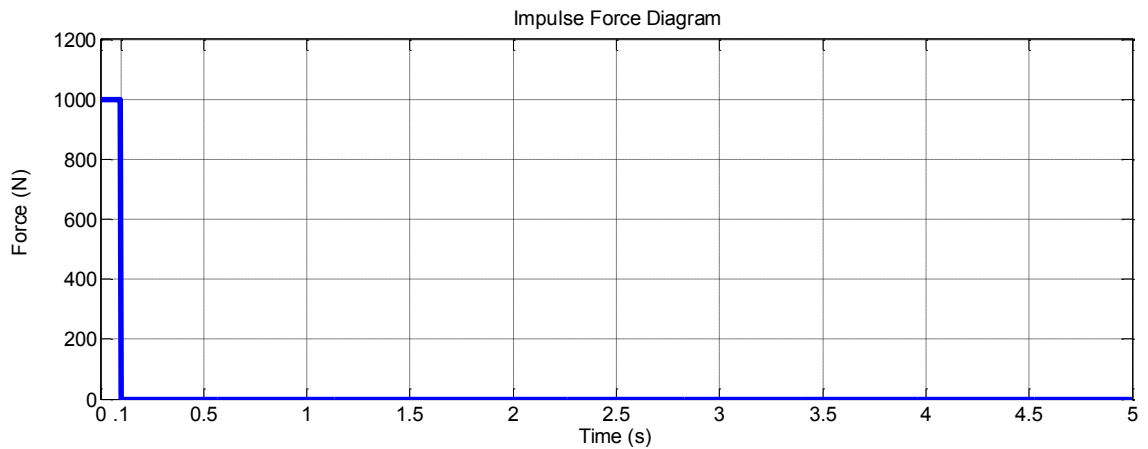
Figure 3-2: Impulse force diagram applied on node C

The node D acceleration results are obtained by the developed FE model in ANSYS and MATLAB are also shown in Figures 3-3 and 3-4, respectively. A comparison

between Figures 3-3 and 3-4 shows the good conformity of ANSYS results, and the built

Matlab model. This validates the structural dynamics modeling code as well.
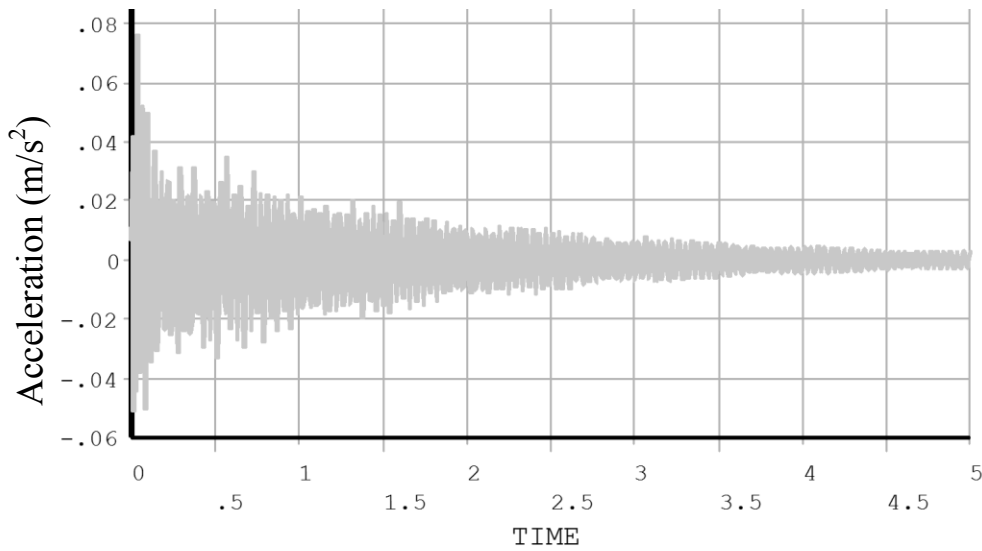
Figure 3-3: Acceleration response of node D due to impulse force exerted on node C –
result is calculated by ANSYS
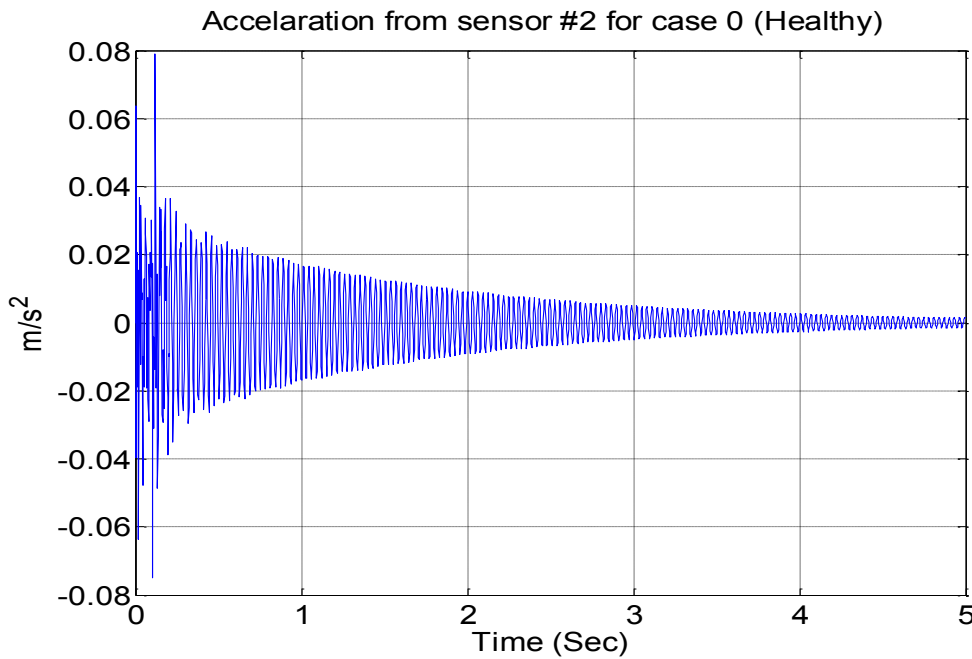
Figure 3-4: Acceleration response of node D due to impulse force exerted on node C –
result is calculated by MATLAB

3.4　Frequency response function

In section 2.4, the Frequency Response Function (FRF) is described in details. The FRF is required to find the optimum arrangement of sensors. The installed sensor positions are shown in Figure 3-5 and the six different FRF responses are indicated in Figures 3-6 to 3-11.

The FRF corresponding to each sensor will be derived from equation (2.17) as:

$$H_1(f) = \frac{S_{uy}(f)}{S_{uu}(f)} = \frac{Y(f)\bar{U}(f)}{U(f)\bar{U}(f)} \tag{3-1}$$

Where $\bar{U}(f)$ is the complex conjugate of the $U(f)$ and Y and U are fast Fourier transforms of $y(t)$ and $u(t)$.
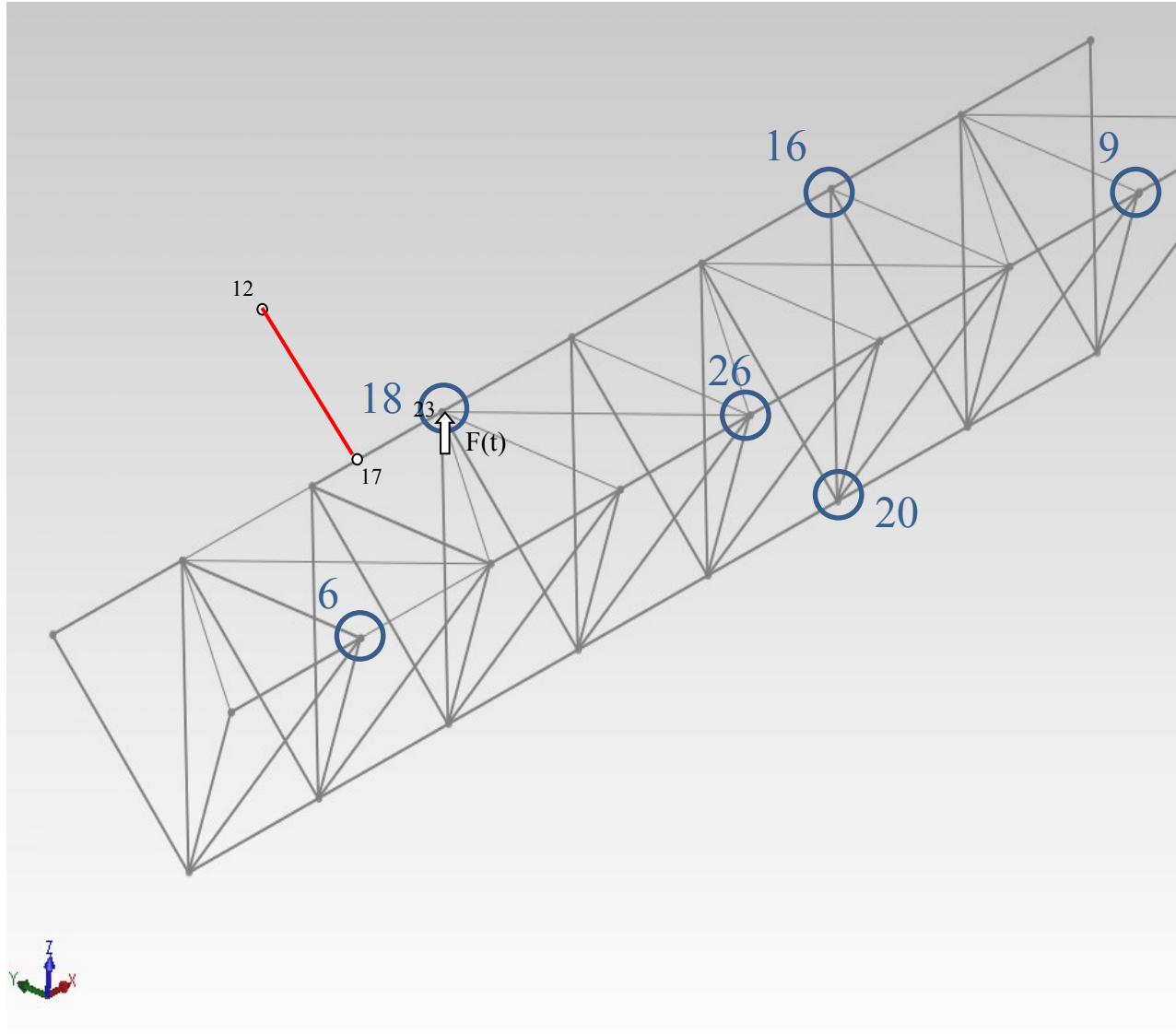
Figure 3-5: Sensor and actuator locations and their equivalent node number. Damaged member 12-17
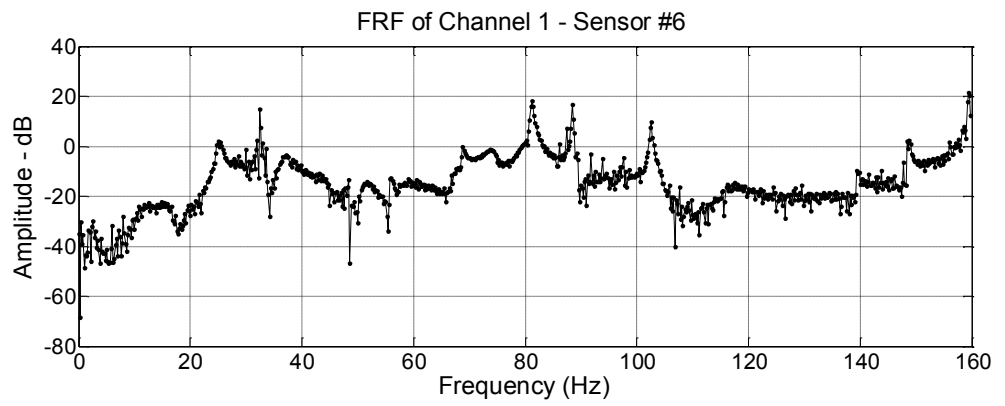
Figure 3-6: FRF from sensor #6 and actuator #23
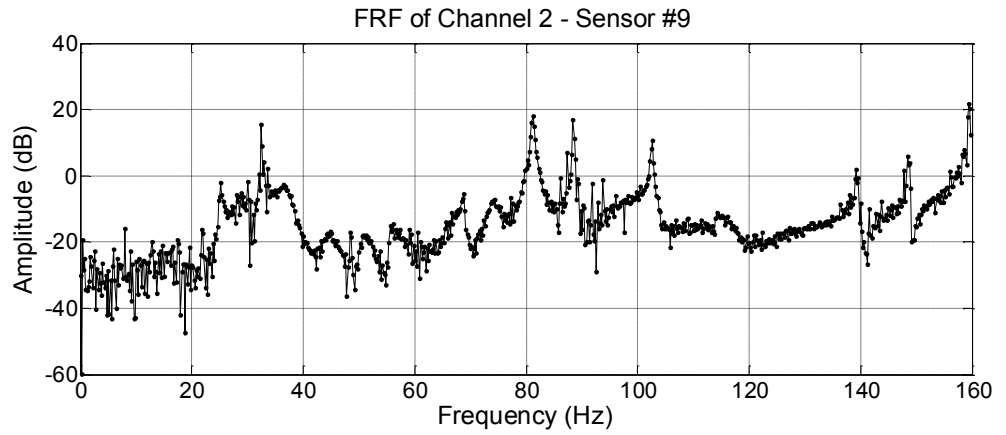
Figure 3-7: FRF from sensor #9 and actuator #23
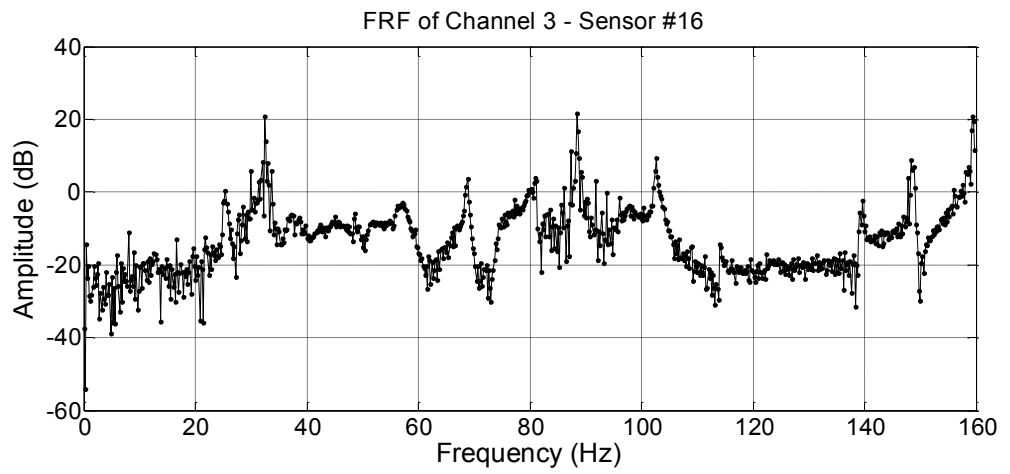
Figure 3-8: FRF from sensor #16 and actuator #23

FRF of Channel 4 - Sensor #18
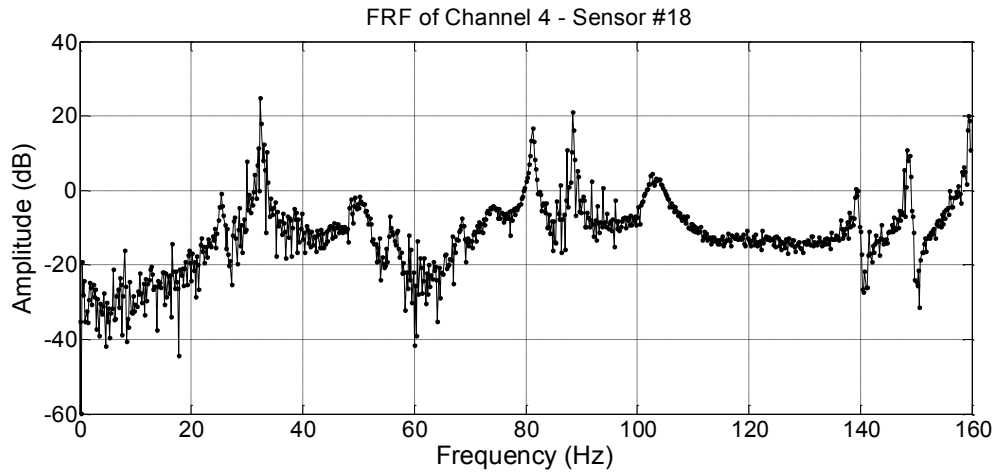
Figure 3-9: FRF from sensor #18 and actuator #23

FRF of Channel 5 - Sensor #20
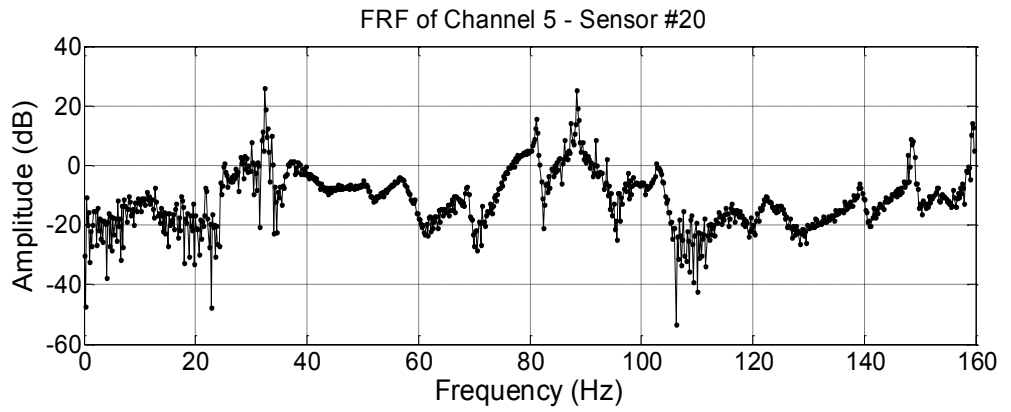
Figure 3-10: FRF from sensor #20 and actuator #23

FRF of Channel 6 - Sensor #26
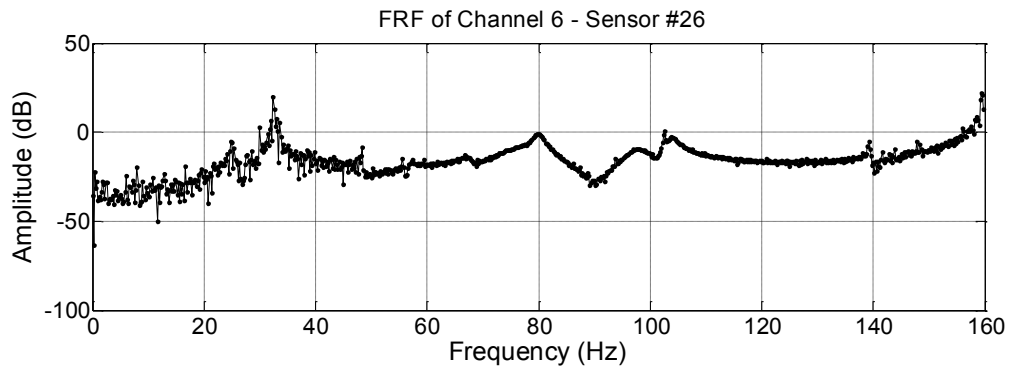
Figure 3-11: FRF from sensor #26 and actuator #23

If a known member of the truss is damaged, there will be a change in the FRF response of all sensors. Let say the member connecting nodes 12 and 17 in Figure 3-5 is damaged. To model the damage it is assumed that the cross section area of this member is reduced by 20%. This means a crack of size 10 mm as shown in Figure 3-12.
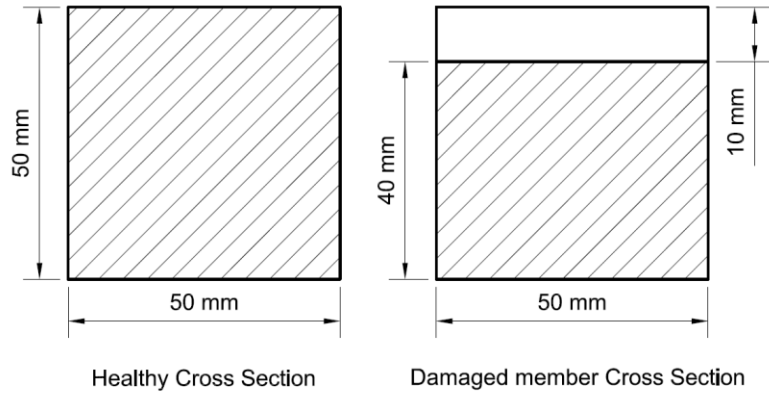
Figure 3-12: Cross section of healthy and damaged truss member

Figure 3-13 indicates the FRF response of the healthy and damaged truss from sensor #6 together. It is clear that these responses are slightly different. This difference is employed to define the objective function of sensor arrangement problem in the next section.
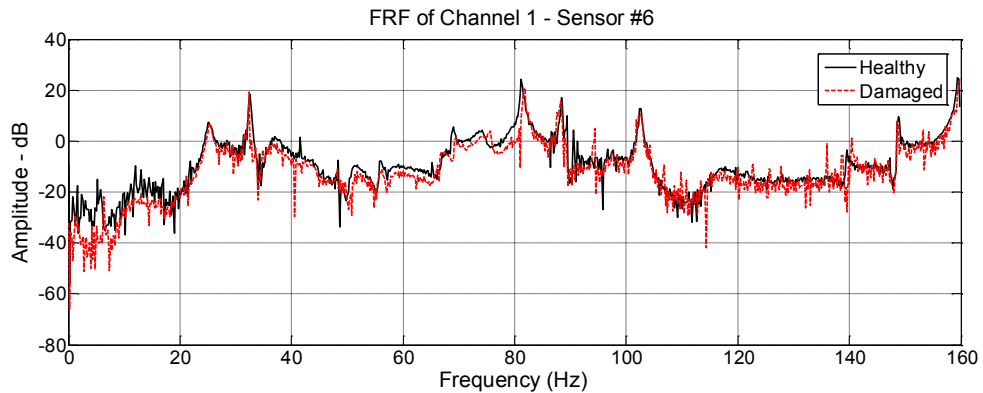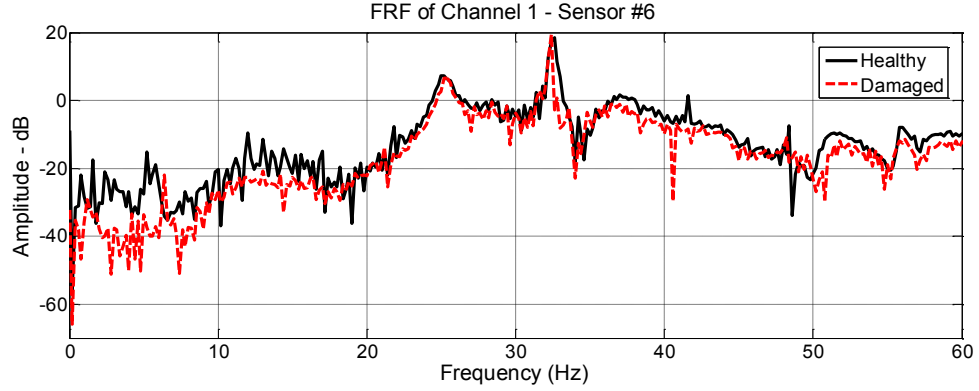
Figure 3-13: Top - FRF from sensor #6 and actuator #23 for healthy and damaged member connecting nodes 12 and 17 , Bottom – Zooming to frequencies 0-60 Hz

3.5   Sensor arrangement optimization

In section 2.5 the problem formulation for sensor arrangement optimization is presented. In this section the formulation has been applied to the space truss structure investigated in this study. The specific member designated by nodes 12 and 17 in Figure 3-5 is supposed to be damaged member. The damage is modeled by 20% reduction in cross section area (Figure 3-12). The problem is to find the optimum sensor arrangement to capture and detect this damage as accurate as possible.

The problem formulation has been recast here again for the sake of clarity.

$$Minimize \ f^{j}(p,M) = \left\| \frac{F_v(p,j) - R_v(p,M,j)}{F_v(p,j)} \right\|$$

(3-2)

$$Subject \ to : M \subset \{1,2,...,N\}, \quad 0 \le p \le 1$$

Where

$$F_v(p,j) = \sum_{i=1}^{N} \left| \frac{H_i(f) - H_i^j(f,p)}{H_i(f)} \right|$$

$$(3\text{-}3)$$

$$R_v(p,M,j) = \sum_{i \in M \neq \varnothing} \left| \frac{H_i(f) - H_i^j(f,p)}{H_i(f)} \right|$$

The number of sensors which their arrangement is to be optimized is selected to be six. The starting sensor configuration is the same as presented in Figure 3-5

$$X_0 = \{6, 9, 16, 18, 20, 26\} \tag{3-4}$$

The MVPS algorithm is employed in NOMADm software which is a free package written in MATLAB [71]. It addresses MVPS and its applications in a very compact and efficient way. The strength of the program is that the design variables could be string types rather than numbers. For example NOMADm is employed to solve the problem of optimization of the number and composition of heat intercepts in a thermal insulation system [72].

Starting from the initial set X_0 in (3-4) and 3 other starting sets the objective function has been minimized. Figure 3.14 shows the iteration history for different initial points. As it can be realized the problem is multimodal and contains different local minima. It should be noted that this is a combinatory optimization problem and there are $\binom{26}{6} = \frac{26!}{20! \times 6!} = 230230$ possible combinations. Thus it would be computationally very expensive to investigate all using brute-force approaches. The optimum set has been found to be $X^* = \{6, 7, 9, 16, 17, 23\}$. It should be noted that this set is the best sensor location set to capture the damage in a particular member (in this case member

connecting nodes 12 and 17). This approach could be suggested when there is a critical member to be monitored and the SHM approach may be tailored to prevent structure failure in that member.
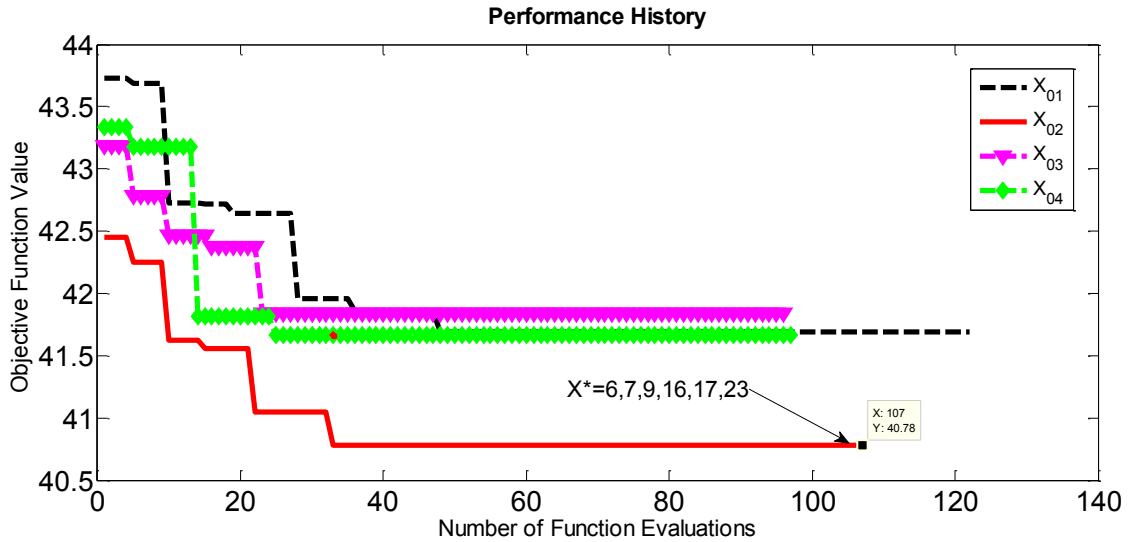
Figure 3-14:Objective function value versus number of function evaluation using four different starting sets

3.6   Damage sensitive feature extraction

In 2.6 the damage sensitive features (DSFs) and Damage Index (DI) are discussed. Here these features are extracted and discussed for the space truss structure investigated in this study. In this section the DIs for the truss structure with optimum sensor set $X^* = \{6,7,9,16,17,23\}$ is extracted. The dynamic force is applied on node #23.

Figure 3-15 indicates the truss structure with all node numbers and optimum sensor set X^* positions. Results for different damage location are presented. It should be noted that only one member is presumed damaged per each simulation run. The crack size is

assumed to be 10 mm causing 20% cross section area reduction in members ①, ②, ③, ④, ⑤ (see Figure 3-15).
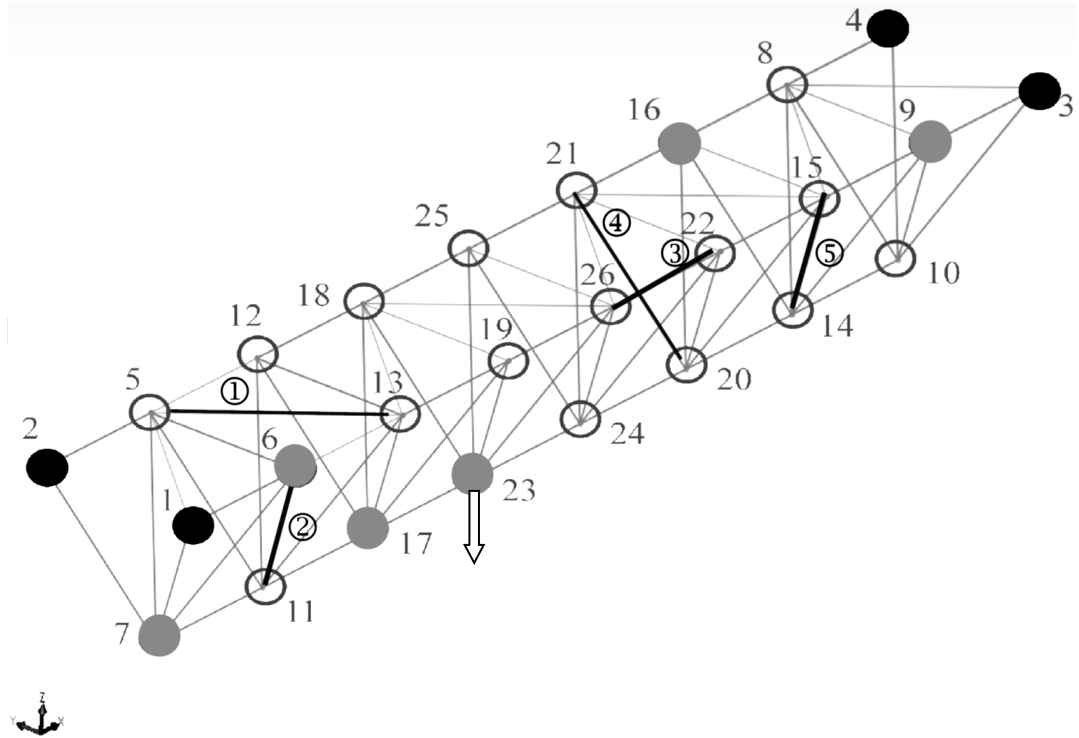
Figure 3-15: Truss structure with 4 clamped nodes (1-4), sensor set $X^* = \{6, 7, 9, 16, 17, 23\}$, studied damaged cases, and loaded node 23

The DI diagrams are indicated in the following Figures. Since there are six installed sensors, six DI diagram is generated. Each diagram studies 10 different cases including 5 healthy cases and 5 damaged cases as discussed in Chapter 2. Each bar in these Figures represents the standard deviation from the base line data. Apparently DI for damaged cases is much higher than the threshold which was defined in Equation (2.9).
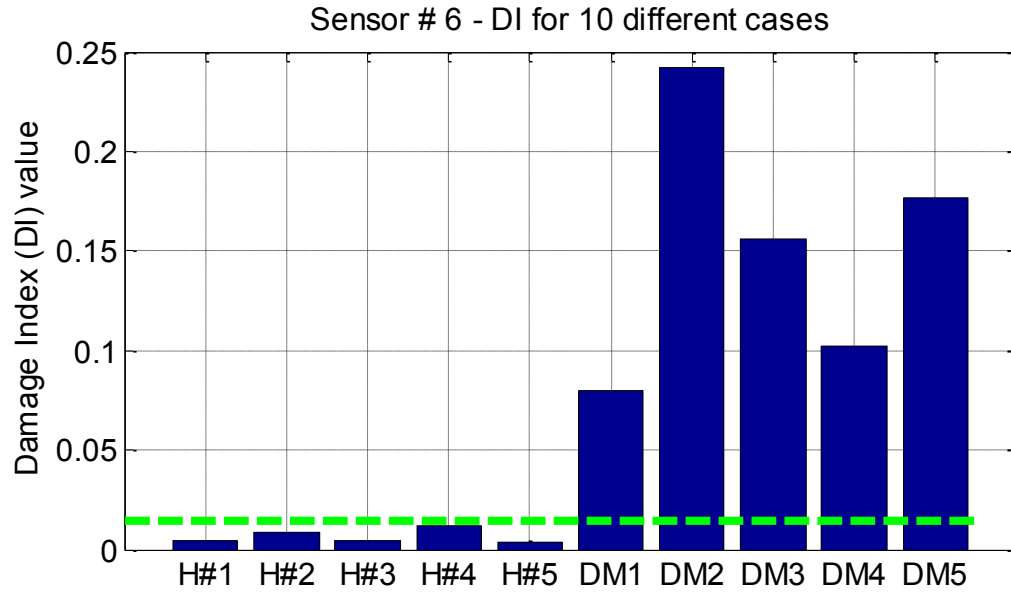
Figure 3-16: DI for each healthy case (H),and damaged cases (DM) obtained from sensor #6
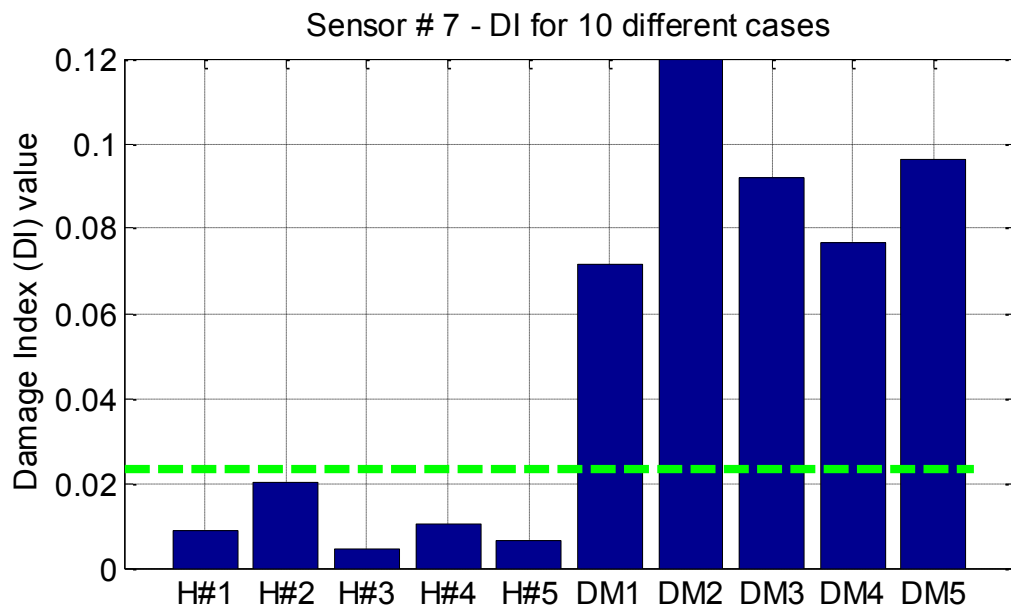
Figure 3-17: DI for each healthy case (H), and damaged cases (DM) obtained from sensor #7
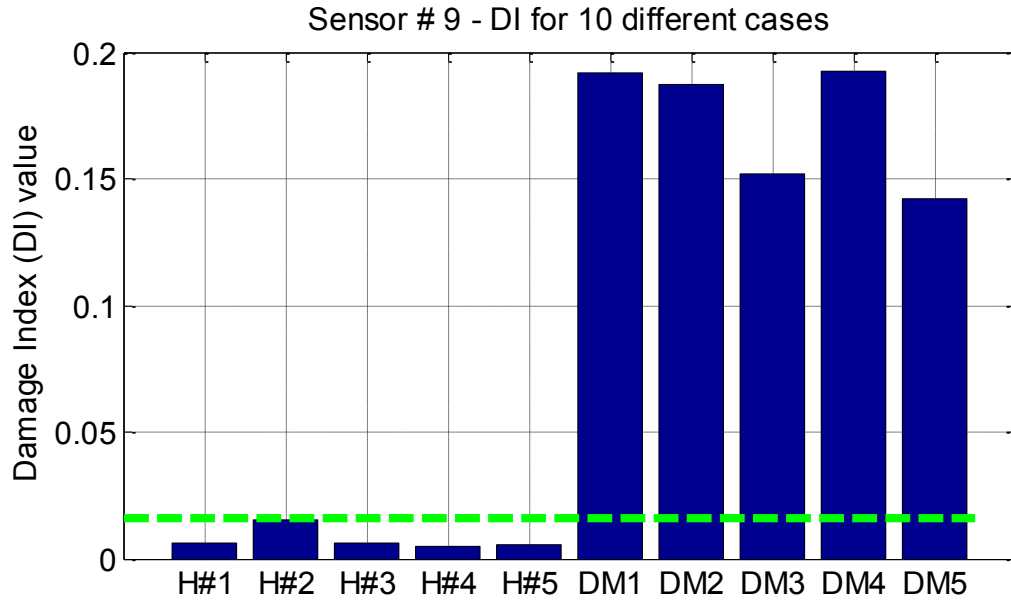
Figure 3-18: DI for each healthy (H), and damaged (DM) cases obtained from sensor #9
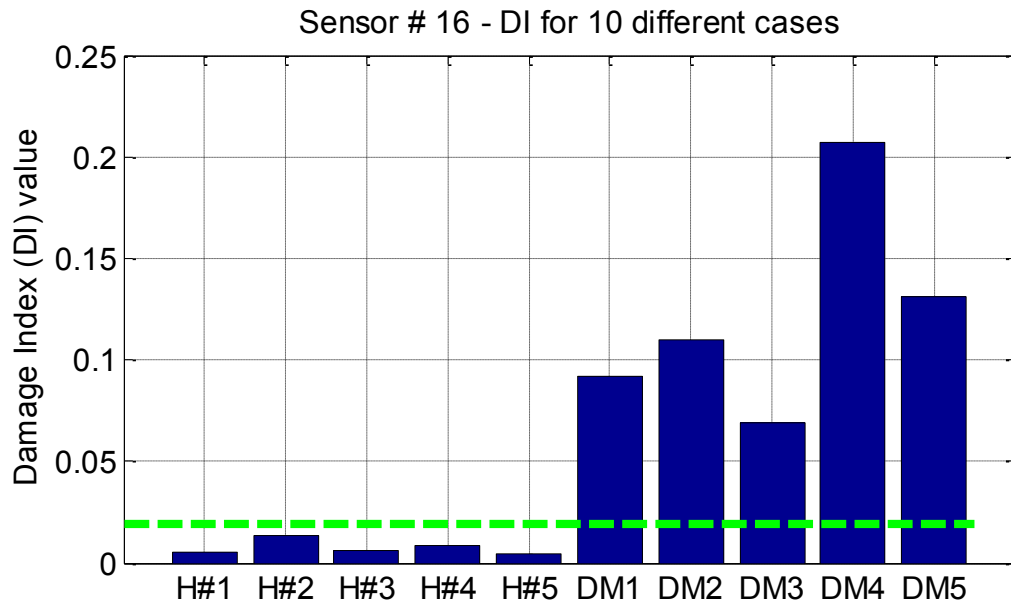
Figure 3-19: DI for each healthy (H), and damaged (DM) cases obtained from sensor #16
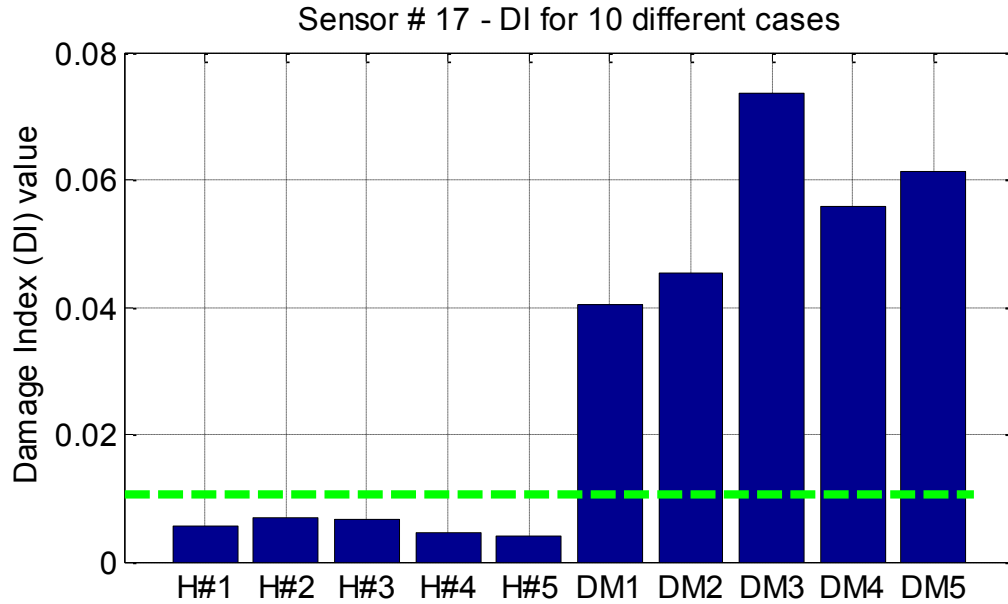
Figure 3-20: DI for each healthy (H), and damaged (DM) cases obtained from sensor #17
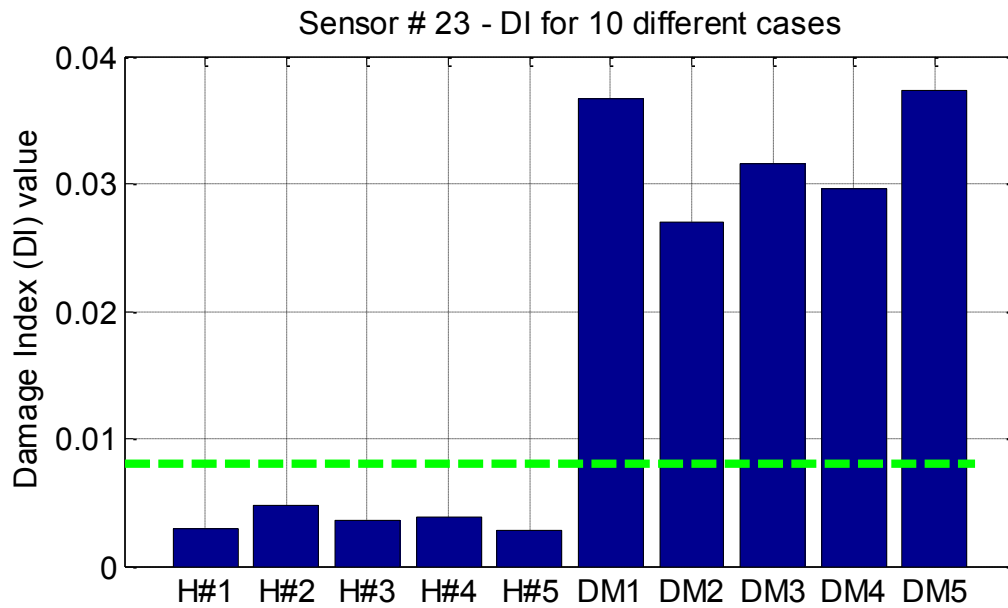
Figure 3-21: DI for each healthy (H), and damaged (DM) cases obtained from sensor #23

As it can be realised damage can be easily identified using formulated damage index (DI). It is interesting to note that information from each sensor could be used to

identify the existence of the damage. Thus defined DI in Eq. 2.9 proved very powerful in discriminating among healthy and damaged cases.

Once the damage is identified, the next important step in SHM is to exactly locate the damage for accurate diagnosis. The level of severity of the damage is also of great importance. These topics are addressed in Section 2.8 and here the results are presented in the following section.

3.7   Damage localization results

Damage localization is the final part of the proposed SHM package. It means isolating the faulty member among all truss structure members and reporting the damage location by its pre allocated member number. As it is discussed in more detail in section 2.8, a tool called LibSVM [69] is employed to localize the damage in the truss structure.

LibSVM needs a training data set. In the space truss structure addressed here, the Damage Sensitive Features (DSFs) are AR parameters. Unlike the damage detection phase which could be performed with the help of only one sensor, to localize the damage, all information from all sensors is required. DSFs are assembled into a matrix namely Damage Sensitive Matrix (DSM).

$$DSM^{(i)} = \begin{bmatrix} DSF_1^T \\ DSF_2^T \\ \vdots \\ DSF_6^T \end{bmatrix}^{(i)} = \begin{bmatrix} AR_{1,1} & AR_{1,2} & . & . & . & AR_{1,6} \\ AR_{2,1} & AR_{2,2} & . & . & . & AR_{2,6} \\ . & & . & & & . \\ . & & . & & & . \\ . & & . & & . & . \\ AR_{20,1} & AR_{20,2} & . & . & . & AR_{20,6} \end{bmatrix}^{(i)} , \quad i = 1,2,...,NR \qquad 3\text{-}5)$$

Each column of the DSM matrix is a feature vector corresponding to a sensor which is numbered by the column number. The number of DSM matrix columns is equal to the number of installed sensors and NR is the number of realization. By try and error it is found that NR=10 provides acceptable results.

The training data set must be assembled in a special format to be used in the LibSVM tool. All possible damage locations should be taken into account. For each damage case, there are NR DSM matrices. Since only one damaged member is considered to occur at a time, so total of 70 different cases plus one healthy case is studied. Note that the 3D truss in Figure 3-15 has 70 members. So the training data set is the assembly of $71 \times 10 = 710$ DSM matrices which are properly labeled.

Figure 3-22 shows the DSM matrix diagram for the studied truss structure. This is the combined format of Figures 2-15 to 2-20 for another set of sensors.
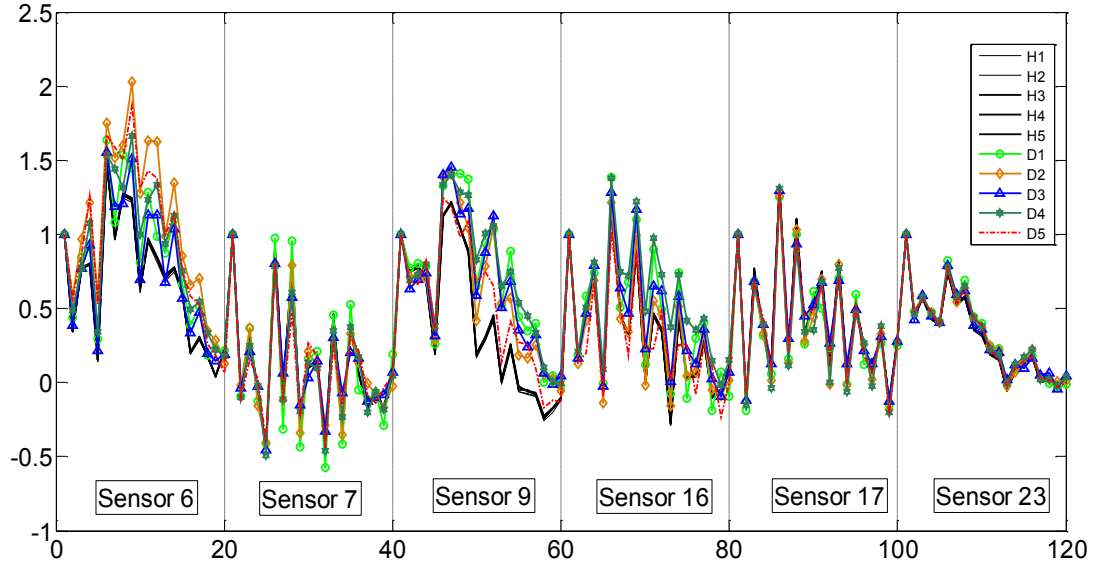
Figure 3-22: AR parameters (DSFs) of truss structure with 6 installed sensors at $X^* = \{6,7,9,16,17,23\}$ forming the DSM matrix (combination of Figures 2-15 to 2-20 for another configuration of sensors)

The training data set is assembled in a `text` file with a special format indicated in Figure 3-23. It is interesting to note that since all AR parameter vectors for each sensor starts with 1, and hence is a common value among all DSM matrix columns, it is better to eliminate it from each DSF vector. The reason is that it will help to maximize the correlation among different categories by eliminating common elements.

The selected AR parameter order is 20 and the number of sensors is 6, hence there are 120 elements in each DSM matrix. It is clear from Figure 3-23 that each row has 119 (starting from index 0) AR parameter values instead of 120. The missing one is the common value 1 which is eliminated from each DSF vector. Case label 0 corresponds to the healthy case and other labels correspond to the damaged member numbers.

After feeding the training data set to the LibSVM program, a trained model is generated. This model is used to predict the test signals and finding out which signal

(with unknown label) belongs to which case label. The generated test signals cover all possible damage places, i.e. 70 members.
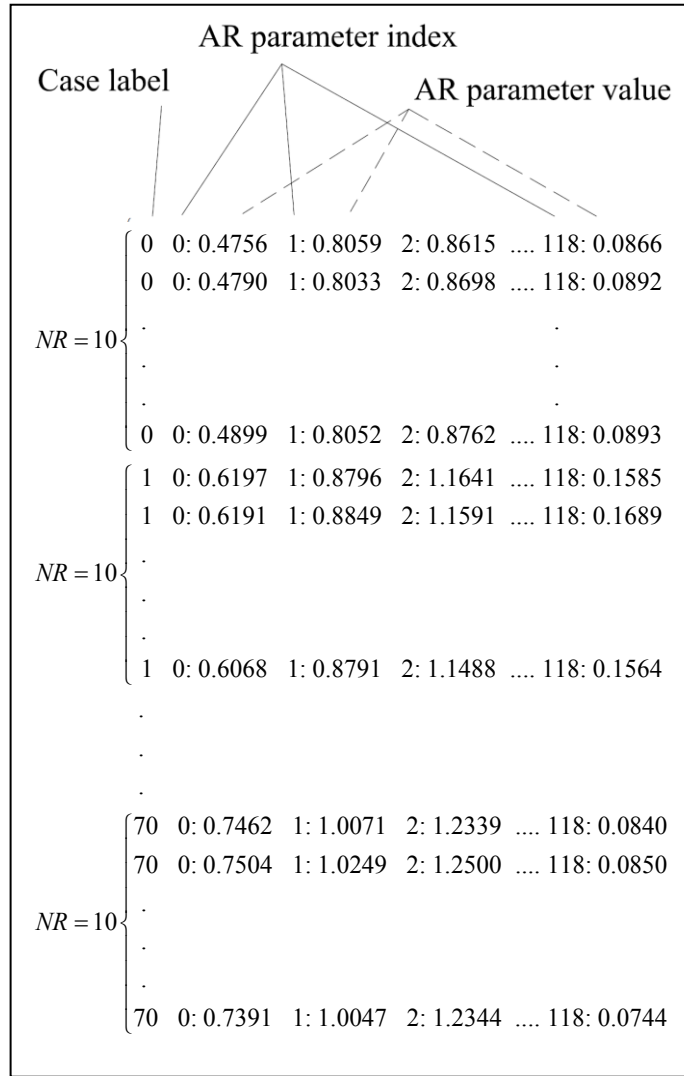
Figure 3-23: Training data set text file format

Table 3-2 indicates both the successful and the wrong predictions, for the damage size of 10 mm in each member at a time. Also the percentage of successful predictions is calculated and reported as the True Prediction Index (TPI).

Table 3-2: Localization results for the 3D truss with a crack size of 10mmand applied force on node #23

DM	Predicted	DM	Predicted	DM	Predicted	DM	Predicted
0	0	18	64	36	36	54	54
1	1	19	8	37	37	55	55
2	2	20	20	38	38	56	56
3	3	21	21	39	0	57	57
4	4	22	22	40	40	58	58
5	5	23	23	41	41	59	59
6	6	24	24	42	42	60	60
7	7	25	25	43	43	61	61
8	1	26	26	44	1	62	62
9	58	27	27	45	45	63	63
10	10	28	28	46	46	64	64
11	11	29	29	47	47	65	65
12	12	30	30	48	48	66	66
13	13	31	31	49	49	67	65
14	14	32	32	50	50	68	68
15	65	33	33	51	51	69	69
16	20	34	34	52	52	70	70
17	17	35	35	53	53	TPI=61/71=85.9%	

3.8 Sensitivity analysis

Sensitivity analysis has been conducted to investigate the sensitivity of the proposed SHM package results to different crack sizes, applied force locations, number of installed sensors and AR parameter order number. In this section the change in each of these parameters are studied and their effect in the results is explored.

3.8.1 Sensitivity to crack size

A range of crack sizes from 1mm to 25 mm (half the cross section height) is studied and the detection and localization TPIs are investigated. Figure 3-24 indicates the detection rate versus crack size in mm. As it can be realized, if the crack size is more than 2 mm then the detection rate is successful in at least 84% of conditions.

79
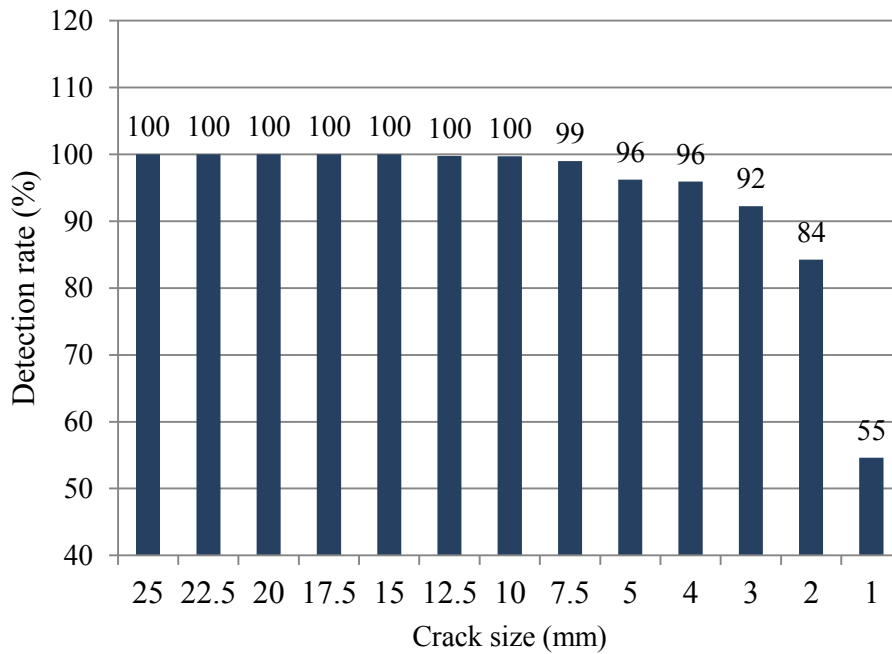
Figure 3-24: Sensitivity of the detection phase to crack size

Figure 3-25 is the sensitivity of the localization phase to crack size parameter. It can be seen that if the crack size is 18 mm in around 90% of times the damage locations are predicted successfully. If the crack size is about 13.7 mm, 70% of attempts to locate the damage are successful. Figure 3-26 is the same as Figure 3-25 except the damage is represented as the percentage of cross section.
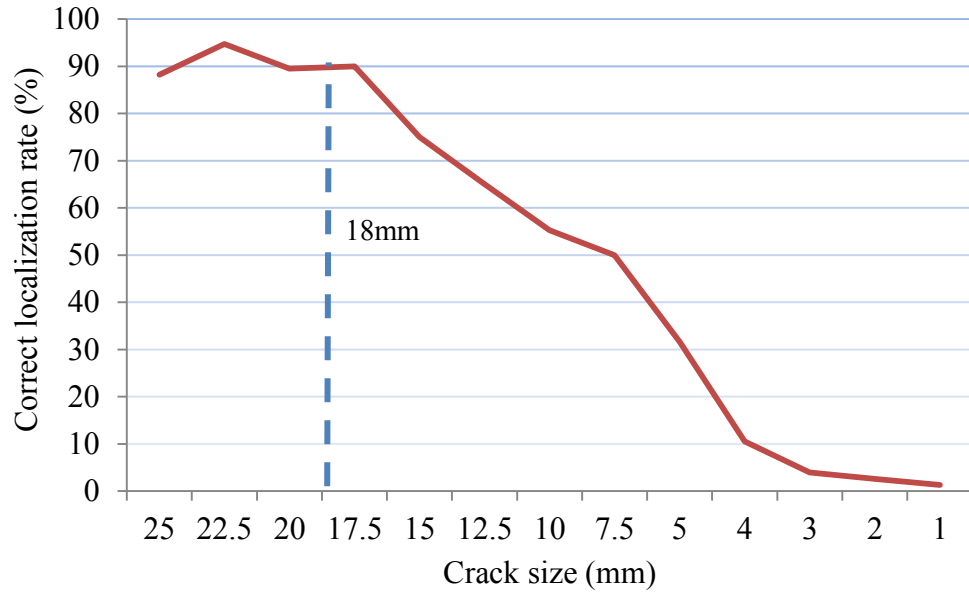
Figure 3-25: Sensitivity of localization phase to crack size in mm
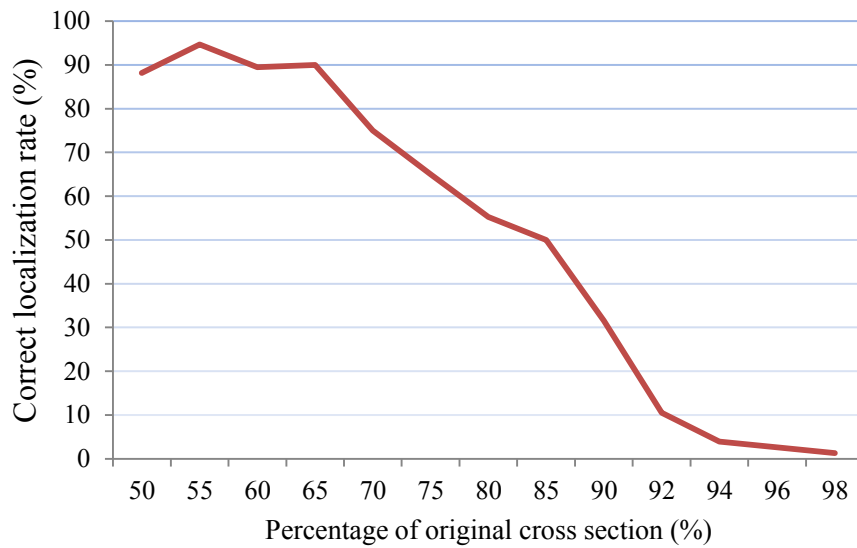
Figure 3-26: Sensitivity of localization phase to crack size in percentage of original cross section~

Since the nature of the problem is not linear, the correct localization rate is not decreasing continuously in all incidents.

3.8.2   Sensitivity to applied force location

Let us consider the space truss structure in Figure 3-15. In all previous results, the force is applied on node #23. In this section the effect of changing applied force location is studied. Assume that force is also applied on nodes {7, 11, 17, 23, 24, 20, 14, 10} and the crack size is *18mm*. Also the installed sensors are those at location $X^* = \{6,7,9,16,17,23\}$.

The detection as expected is found correctly in 100% of times as expected in all cases. The localization diagram is shown in Figure 3-27. It can be concluded that the force location on nodes #20 and #14 gives slightly better results in localization than other excitation locations.
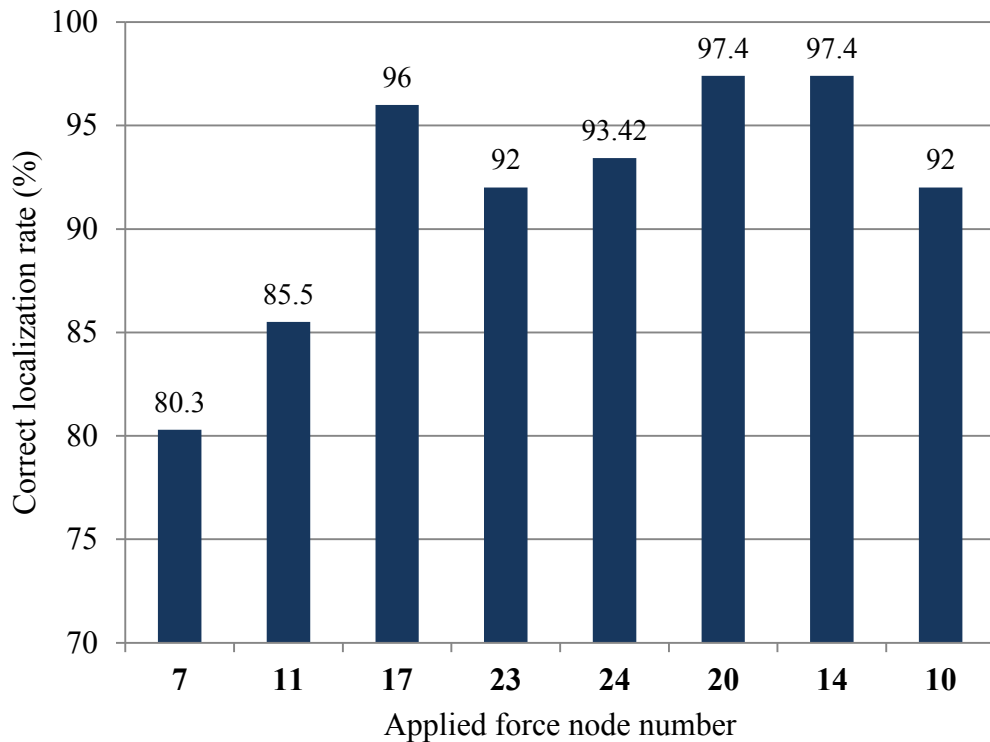
Figure 3-27: TPI versus applied force location number

3.8.3 Sensitivity to the number of installed sensors

The results of this section could be of great importance, due to interests to minimize the required sensors. Sensors, data acquisition and communication with the central computer are always a complex and expensive task. Detection phase can be done by only one sensor, but the localization phase requires a set of sensors to categorize the signals considering the trained model of damaged cases. Let us assume that the damage size is 10 mm, the loaded node is node #23 and AR parameter order is 20. The sensors are added in the sequence of $X = \{6,7,9,16,17,23,8,14,11,20,13\}$ one after another. The best localization accuracy to the selected configuration is found to be with 8 sensors. The SVM method fails to report better results with more number of sensors and incidents of wrong categorizations increase.
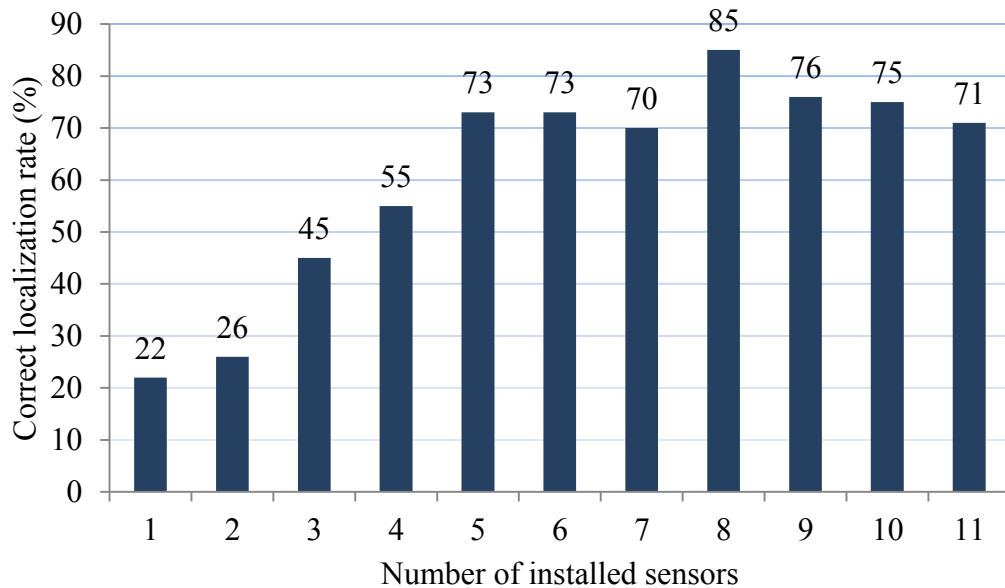
Figure 3-28: Sensitivity of damage localization technique to the number of installed sensors – the sensors are installed at locations $X = \{6,7,9,16,17,23,8,14,11,20,13\}$ one after another

3.8.4 Sensitivity to AR parameter order

The last parameter that is studied in the sensitivity analysis concept is the AR parameter order. This order affects the DSM matrix dimension and the feature vector length. Figure 3-29 shows the correct localization rate versus the AR order. The crack size is assumed to be 18mm and the loaded node is node #23. The 18mm crack size is selected because at this crack size, the number of correct localized damaged members is 90% and good enough to study the effect of other parameters. There are six installed sensors on the truss structure at optimum location $X^* = \{6,7,9,16,17,23\}$. AR orders ranging from 15 to 20 give the best results as it can be seen from Figure 3-29.

It should be mentioned that the detection rate is again 100% in all cases except is AR order=5 which is 85%.
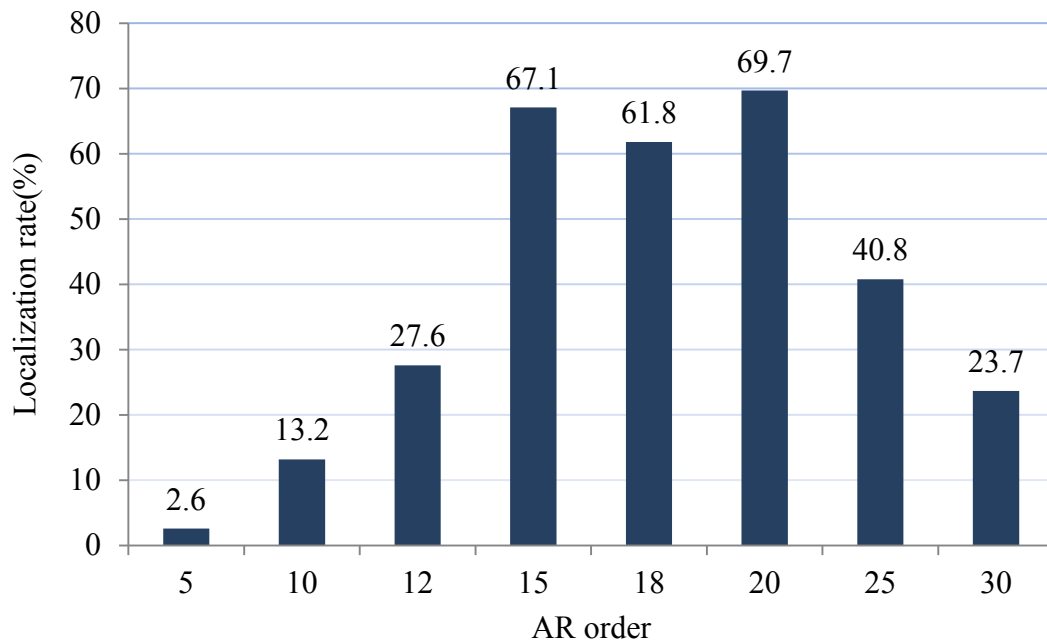
Figure 3-29: Sensitivity of damage localization technique to the AR order parameter

CHAPTER 4

CONCLUSION AND FURTHER STUDIES

4.1 Conclusion

Improving safety, costs of inspection procedure, probable significant damage in expensive structures due to failure in a small member, man-hour required to do inspection, monitoring and consequent costs are some of the reasons that have attracted researchers in the field of SHM. In this thesis, an efficient SHM methodology to detect and localize the single damage in truss structures has been proposed. However the study is not limited to truss structures. It can be extended to frame and plate type structures easily.

The concept of SHM is explained and a method is proposed for the detection of damages based on Auto Regressive (AR) parameters. AR parameters of order p are simply a set of parameters that estimate each term of a sequence in terms of p previous terms of the same sequence of numbers. It turns out that AR parameters are damage sensitive features.

The AR parameters of a healthy case are assumed to be the baseline data which is a reference to judge other cases. A Damage Index is defined to be the standard deviation of any other unknown signal from this baseline data. This unique index is a very powerful tool to detect the damage in the structure.

The localization process is more complex. It needs data classification techniques which are ranging from genetic algorithm, neural networks to Support Vector Machine (SVM). SVM is an statistical technique which is used in this research. It can successfully classify different signals extracted from a 3D sample truss structure. Localization requires a rich source of simulated data. If the simulation is done perfectly, a large set of simulated data is used to feed the classifier (SVM in here) to develop the trained model. This model is then subsequently used to predict the unknown signals and find the most correlated "known" category and report the case label as the best match for the "unknown" signal. This is called the localization process.

At the end an extensive sensitivity analysis is performed to study the effect of parameter changes to the detection and localization processes. It should be mentioned that all results are case dependent and performed for the sample truss structure.

4.2 Further studies

This study can be extended in the following areas

1) Different type of structures like frames and plates or a combination of both could be studied. Also composite materials could be a good candidate.

2) In this study damage is applied on only one member at a time, a good extension could be the study of multiple damage occurrences at a time.

3) Other damage types other than crack could be studied. Loosened bolts, high temperature spots and the resulting thermal stresses, delamination of composite materials and corrosion are a handful of other damage types.

REFERENCES

1. Banerjee, S., et al., *A wave propagation and vibration-based approach for damage identification in structural components.* Journal of Sound and Vibration, 2009. **322**(1): p. 167-183.

2. Sohn, H., et al., *A review of structural health monitoring literature: 1996-2001.* 2004: Los Alamos National Laboratory Los Alamos,, New Mexico.

3. Staszewski, W., C. Boller, and G.R. Tomlinson, *Health monitoring of aerospace structures: smart sensor technologies and signal processing.* 2004: Wiley.

4. Bently, D.E., C.T. Hatch, and B. Grissom, *Fundamentals of rotating machinery diagnostics.* 2002: Bently Pressurized Bearing Press.

5. Giurgiutiu, V., *Structural health monitoring: with piezoelectric wafer active sensors.* 2007: Academic Press.

6. Balageas, D., *Introduction to structural health monitoring.* 2006: Wiley Online Library.

7. Sampaio, R., N. Maia, and J. Silva, *Damage detection using the frequency-response-function curvature method.* Journal of Sound and Vibration, 1999. **226**(5): p. 1029-1042.

8. Liao, J., et al., *Finite Element Model Updating Based on Field Quasi-static Generalized Influence Line and Its Bridge Engineering Application.* Procedia Engineering, 2012. **31**(0): p. 348-353.

9. Moaveni, B., et al., *Finite element model updating for assessment of progressive damage in a three-story infilled RC frame.* Journal of Structural Engineering, 2012.

10.   Song, W., S. Dyke, and T. Harmon, *Application of Nonlinear Model Updating for a Reinforced Concrete Shear Wall.* Journal of Engineering Mechanics, 2012. **139**(5): p. 635-649.

11.   Lifshitz, J.M. and A. Rotem, *Determination of reinforcement unbonding of composites by a vibration technique.* Journal of Composite Materials, 1969. **3**(3): p. 412-423.

12.   Cawley, P. and R. Adams, *The location of defects in structures from measurements of natural frequencies.* The Journal of Strain Analysis for Engineering Design, 1979. **14**(2): p. 49-57.

13.   Kessler, S.S., *Piezoelectric-based in-situ damage detection of composite materials for structural health monitoring systems*. 2002, Massachusetts Institute of Technology.

14.   Srinivasan, M. and C. Kot, *Effect of damage on the modal parameters of a cylindrical shell*. 1992, Argonne National Lab., IL (United States).

15.   Pandey, A., M. Biswas, and M. Samman, *Damage detection from changes in curvature mode shapes.* Journal of sound and vibration, 1991. **145**(2): p. 321-332.

16.   Farrar, C.R., S.W. Doebling, and D.A. Nix, *Vibration–based structural damage identification.* Philosophical Transactions of the Royal Society of London. Series A: Mathematical, Physical and Engineering Sciences, 2001. **359**(1778): p. 131-149.

17.   Stubbs, N., J.-T. Kim, and C. Farrar. *Field verification of a nondestructive damage localization and severity estimation algorithm*. in *Proceedings-SPIE the international society for optical engineering*. 1995: SPIE international society for optical engineering.

18.   Kim, J.-T., et al., *Damage identification in beam-type structures: frequency-based method vs mode-shape-based method.* Engineering structures, 2003. **25**(1): p. 57-67.

19.   Carden, E.P. and P. Fanning, *Vibration based condition monitoring: a review.* Structural Health Monitoring, 2004. **3**(4): p. 355-377.

20.   Salawu, O.S. and C. Williams, *Bridge assessment using forced-vibration testing.* Journal of structural engineering, 1995. **121**(2): p. 161-173.

21.   Alampalli, S., G. Fu, and E.W. Dillon, *Signal versus noise in damage detection by experimental modal analysis.* Journal of structural engineering, 1997. **123**(2): p. 237-245.

22.   Zagrai, A.N. and V. Giurgiutiu, *Electro-mechanical impedance method for crack detection in thin plates.* Journal of Intelligent Material Systems and Structures, 2001. **12**(10): p. 709-718.

23.   Lange, I., *Characteristics of the impedance method of inspection and of impedance inspection transducers.* Soviet Journal of Nondestructive Testing, 1979. **14**(11): p. 958-966.

24.   Cawley, P., *The impedance method of non-destructive inspection.* NDT international, 1984. **17**(2): p. 59-65.

25.   Dragan, K., *Image Processing approach for the Non Destructive Evaluation (NDE) of the composite materials as the input to structural durability assessment.* Data processing, 2011. **50**: p. 256.

26.   Marsh, B.J., et al., *System and method for automated inspection of large-scale part.* 2010, Google Patents.

27.   DRAGAN, K., et al. *Structural Integrity Monitoring of Wind Turbine Composite Blades with the Use of NDE and SHM Approach*. in *Proceedings of the Fifth European Workshop on Structural Health Monitoring 2010*. 2010: DEStech Publications, Inc.

28.   Holford, K., et al., *Acoustic emission for monitoring aircraft structures.* Proceedings of the Institution of Mechanical Engineers, Part G: Journal of Aerospace Engineering, 2009. **223**(5): p. 525-532.

29.   Yan, T. and B. Jones, *Traceability of acoustic emission measurements using energy calibration methods.* Measurement Science and Technology, 2000. **11**(11): p. L9.

30.   Wevers, M., *Listening to the sound of materials: acoustic emission for the analysis of material behaviour.* NDT & E International, 1997. **30**(2): p. 99-106.

31. Ovanesova, A. and L. Suarez, *Applications of wavelet transforms to damage detection in frame structures.* Engineering structures, 2004. **26**(1): p. 39-49.

32. Sundararaman, S., *Numerical and experimental investigations of practical issues in the use of wave propagation for damage identification*. 2007: ProQuest.

33. Su, Z., L. Ye, and Y. Lu, *Guided Lamb waves for identification of damage in composite structures: A review.* Journal of sound and vibration, 2006. **295**(3): p. 753-780.

34. Harri, K., P. Guillaume, and S. Vanlanduit, *On-line damage detection on a wing panel using transmission of multisine ultrasonic waves.* NDT & E International, 2008. **41**(4): p. 312-317.

35. Staszewski, W., S. Mahzan, and R. Traynor, *Health monitoring of aerospace composite structures–Active and passive approach.* Composites Science and Technology, 2009. **69**(11): p. 1678-1685.

36. Rose, J.L., *A baseline and vision of ultrasonic guided wave inspection potential.* Transactions-American Society of Mechanical Engineers Journal of Pressure Vessel Technology, 2002. **124**(3): p. 273-282.

37. Worden, K., G. Manson, and D. Allman, *Experimental validation of a structural health monitoring methodology: Part I. Novelty detection on a laboratory structure.* Journal of sound and vibration, 2003. **259**(2): p. 323-343.

38. Kopsaftopoulos, F. and S. Fassois, *Vibration based health monitoring for a lightweight truss structure: Experimental assessment of several statistical time series methods.* Mechanical Systems and Signal Processing, 2010. **24**(7): p. 1977-1997.

39. Trendafilova, I., M. Cartmell, and W. Ostachowicz, *Vibration-based damage detection in an aircraft wing scaled model using principal component analysis and pattern recognition.* Journal of Sound and Vibration, 2008. **313**(3): p. 560-566.

40.   Fassois, S.D. and J.S. Sakellariou, *Time-series methods for fault detection and identification in vibrating structures.* Philosophical Transactions of the Royal Society A: Mathematical, Physical and Engineering Sciences, 2007. **365**(1851): p. 411-448.

41.   Fassois, S.D. and J.S. Sakellariou, *Statistical Time Series Methods for SHM.* Encyclopedia of Structural Health Monitoring, 2009.

42.   Basseville, M., L. Mevel, and M. Goursat, *Statistical model-based damage detection and localization: subspace-based residuals and damage-to-noise sensitivity ratios.* Journal of Sound and Vibration, 2004. **275**(3): p. 769-794.

43.   Mevel, L., M. Goursat, and M. Basseville, *Stochastic subspace-based structural identification and damage detection and localisation—application to the Z24 bridge benchmark.* Mechanical Systems and Signal Processing, 2003. **17**(1): p. 143-151.

44.   Sakellariou, J. and S. Fassois, *Vibration based fault detection and identification in an aircraft skeleton structure via a stochastic functional model based method.* Mechanical Systems and Signal Processing, 2008. **22**(3): p. 557-573.

45.   Kopsaftopoulos, F.P. and S.D. Fassois, *Vibration–based structural damage detection and precise assessment via stochastic functionally pooled models.* Key Engineering Materials, 2007. **347**: p. 127-132.

46.   Beal, J.M., et al., *Optimal sensor placement for enhancing sensitivity to change in stiffness for structural health monitoring.* Optimization and Engineering, 2008. **9**(2): p. 119-142.

47.   Staszewski, W., et al., *Fail-safe sensor distributions for impact detection in composite materials.* Smart Materials and Structures, 2000. **9**(3): p. 298.

48.   Shi, Z., S. Law, and L. Zhang, *Optimum Sensor Placement for Structural Damage Detection.* Journal of Engineering Mechanics, 2000. **126**(11): p. 1173-1179.

49.   Guo, H., et al., *Optimal placement of sensors for structural health monitoring using improved genetic algorithms.* Smart Materials and Structures, 2004. **13**(3): p. 528.

50. Meirovitch, L., *Dynamics and control of structures*. 1990: Wiley New York.

51. Gawronski, W., *Advanced structural dynamics and active control of structures*. 2004: Springer Verlag.

52. Logan, D.L., *A first course in the finite element method*. 2011: Cl-Engineering.

53. Schoukens, J., R. Pintelon, and Y. Rolain, *Mastering system identification in 100 exercises*. 2012: Wiley-IEEE Press.

54. Madisetti, V., *Digital signal processing fundamentals*. 2010: CRC press.

55. Butterworth, S., *On the theory of filter amplifiers.* Wireless Engineer, 1930. **7**: p. 536-541.

56. Schwarz, B.J. and M.H. Richardson, *Experimental modal analysis.* CSI Reliability week, 1999. **36**(3): p. 30-32.

57. Rocklin, G.T., J. Crowley, and H. Vold. *A comparison of H1, H2, and Hv frequency response functions*. in *Proceedings of the 3rd international modal analysis conference, Orlando*. 1985.

58. Figueiredo, E., et al., *Structural health monitoring algorithm comparisons using standard data sets*. 2009, Los Alamos National Laboratory (LANL), Los Alamos, NM (United States).

59. Worden, K., et al., *The fundamental axioms of structural health monitoring.* Proceedings of the Royal Society A: Mathematical, Physical and Engineering Science, 2007. **463**(2082): p. 1639-1664.

60. Devore, J.L., *Probability & Statistics for Engineering and the Sciences*. 2012: Duxbury Press.

61. Yule, G.U., *On a method of investigating periodicities in disturbed series, with special reference to Wolfer's sunspot numbers.* Philosophical Transactions of the Royal Society of London. Series A, Containing Papers of a Mathematical or Physical Character, 1927. **226**: p. 267-298.

62.   Walker, G., *On periodicity in series of related terms.* Proceedings of the Royal Society of London. Series A, 1931. **131**(818): p. 518-532.

63.   Box, G.E., G.M. Jenkins, and G.C. Reinsel, *Time series analysis: forecasting and control*. Vol. 734. 2011: Wiley.

64.   Vapnik, V.N. and S. Kotz, *Estimation of dependences based on empirical data*. Vol. 41. 1982: Springer-Verlag New York.

65.   Vapnik, V., *The nature of statistical learning theory*. 1999: springer.

66.   Vapnik, V., *Statistical learning theory*. 1998, Wiley New York.

67.   Wikipedia. *Support vector machine*. 2013; Available from: https://en.wikipedia.org/wiki/Svm_%28machine_learning%29.

68.   Lafferty, J.D. and G. Lebanon, *Diffusion kernels on statistical manifolds.* 2005.

69.   Chang, C.-C. and C.-J. Lin, *LIBSVM: a library for support vector machines.* ACM Transactions on Intelligent Systems and Technology (TIST), 2011. **2**(3): p. 27.

70.   Chang, C.-C. and C.-J. Lin. 2013; Available from: http://www.csie.ntu.edu.tw/~cjlin/libsvm/.

71.   Mark Abramson. *NOMADm Optimization Software*. 2013; Available from: http://www.gerad.ca/NOMAD/Abramson/nomadm.html.

72.   Kokkolaras, M., C. Audet, and J.E. Dennis Jr, *Mixed variable optimization of the number and composition of heat intercepts in a thermal insulation system.* Optimization and Engineering, 2001. **2**(1): p. 5-29.